

Temperature-Driven Zika Virus Risk Prediction Model and Control Strategies: A Case Study of Brazil

Zongmin Yue*, Xiangrui Ji, Yingpan Zhang

School of Mathematics and Data Science, Shaanxi University of Science and Technology, Xi'an, China

Email: *janna_ym@163.com

How to cite this paper: Yue, Z.M., Ji, X.R. and Zhang, Y.P. (2024) Temperature-Driven Zika Virus Risk Prediction Model and Control Strategies: A Case Study of Brazil. *Journal of Applied Mathematics and Physics*, 12, 4213-4241.

<https://doi.org/10.4236/jamp.2024.1212260>

Received: November 25, 2024

Accepted: December 28, 2024

Published: December 31, 2024

Copyright © 2024 by author(s) and Scientific Research Publishing Inc. This work is licensed under the Creative Commons Attribution International License (CC BY 4.0).

<http://creativecommons.org/licenses/by/4.0/>



Open Access

Abstract

Climate is a major driver of vector proliferation and arbovirus transmission, with temperature being a primary focus of research. Unlike other mosquito-borne diseases, Zika virus transmission involves both sexual transmission between humans and environmental transmission pathways, a characteristic largely overlooked in existing studies. This paper develops a temperature-dependent transmission model based on the unique transmission characteristics of the Zika virus. We estimated the historical transmission of Zika virus in Brazil using a temperature-dependent basic reproduction number to assess the impact of climate change on Zika virus spread in the region. Results indicate that the temperature range for Zika virus outbreaks is between 23.34°C and 33.99°C, peaking at 3.2 at 29.4°C. This range and peak temperature are approximately 1°C lower than those found in models that do not consider environmental transmission pathways. By incorporating seasonal variations into the model and categorizing ten Brazilian cities into five climatic types based on temperature changes, we simulated historical and future daily average temperatures using the GFDL-ESM4 temperature model. We analyzed the control periods and virus risks across different regions and projected Zika virus transmission risk in Brazil under four Shared Socioeconomic Pathways (SSP126, SSP245, SSP370, and SSP585). The results suggest that under the SSP126 scenario, the control periods will extend by 2 - 3 months with rising temperatures. This study concludes by discussing the impact of temperature changes on control measures, emphasizing the importance of reducing adult mosquito populations through the Sterile Insect Technique (SIT) to mitigate future risks.

Keywords

Zika Virus, Basic Reproduction Number, Temperature-Driven, Risk Prediction

1. Introduction

Zika virus, a viral disease transmitted to humans through the bite of infected *Aedes aegypti* mosquitoes, emerged in the Americas in 2015, causing a massive epidemic. Between May and December 2015, about 440,000~1300,000 suspected cases were reported in Brazil alone. Not only that, but Zika virus has spread widely across multiple regions, with 89 countries and territories having reported evidence of Zika virus transmission as of 2016 [1]-[3]. Therefore, it is crucial to predict the spread of Zika virus. The primary vector for the transmission of the Zika virus is the *Aedes aegypti* mosquito. Research indicates that, as small ectothermic organisms, the fitness, life history, and vector capacity of these mosquitoes exhibit a nonlinear and unimodal relationship with environmental temperature. Therefore, temperature is an important driver influencing the population dynamics of *Aedes aegypti* mosquitoes [4]-[6]. Ryan *et al.* [7] applied empirical parametric models of vector transmission of *Aedes aegypti* and *Aedes albopictus* as a function of temperature to predict cumulative monthly global transmission risks in the current climate. Their research shows that under climate change, the scale of the virus transmitted by *Aedes* mosquitoes increases significantly. Carlson *et al.* [8] compiled a spatially explicit global occurrence dataset from Zika virus surveillance and serological surveys and constructed a niche model to map the potential distribution of the virus. Their study indicates that the temperature in areas suitable for Zika virus transmission is higher than that in areas at risk for dengue fever. Tesla *et al.* [9] updated an existing temperatures-dependent basic reproduction model using thermal responses of *Aedes* traits in order to infer the effect of temperature on Zika virus transmission, and their results indicate that the optimal transmission temperature for Zika virus is 29°C. Huber *et al.* [10] extended the SEI-SEIR model for Zika virus to include nonlinear, temperature-dependent vector parameters. They used this model to assess the impact of temperature on the breadth and scale of epidemics. Their research indicates that as temperatures rise, the global range suitable for Zika virus outbreaks will expand, potentially putting a larger proportion of the world's population at risk. Van Wyk *et al.* [11] utilized a temperature-dependent basic reproduction number (R_0) model to predict the risk of Zika virus and dengue viruses in five regions of Brazil. Their model predicted that the R_0 for the Zika virus peaks at approximately 2.7 at around 30.5°C. All of this research suggests that understanding how temperature changes affect Zika virus is important for us to predict and prevent the spread of Zika virus.

It is important to note that unlike viruses such as Japanese encephalitis, malaria, dengue fever, filariasis, Zika virus has a human-to-human transmission pathway in addition to mosquito bite transmission [3] [12], as well as an environmental infection pathway [13]. Environmental infection pathways provide new routes for mosquitoes to contract the virus, which may have led to an underestimation of the Zika virus in previous model assessments. In this paper, we will investigate the impact of climate change on Zika virus based on a new model of temperature-dependent Zika virus transmission in *Aedes aegypti* mosquitoes to obtain the

basic reproduction number related to temperature. Our research extended previous work [9]-[11], in addition to adding environmental infection pathways, as well as analyzing and comparing actual temperatures in ten different Brazilian cities to refine the potential risk of Zika virus outbreaks in different regions. Future annual risk projections are given through five different climate types. In addition, this paper also pays attention to the influence of temperature on the control parameters, and then analyzes the change of the synergistic effect between control measures and temperature.

2. Methods

2.1. Model

The SEIR-SEI compartment modeling framework is used to simulate the transmission of Zika virus. At the same time, we introduced temperature dependence into the model using the fitted thermal response curves of mosquito life history characteristics provided by Mordecai *et al.* [14]. The complete model is:

$$\frac{dS_H}{dt} = \Lambda_H - \beta_H(T)S_H(I_M + \rho I_H) - \mu_H S_H, \quad (1)$$

$$\frac{dE_H}{dt} = \beta_H(T)S_H(I_M + \rho I_H) - (\mu_H + \alpha_H)E_H, \quad (2)$$

$$\frac{dI_H}{dt} = \alpha_H E_H - (\mu_H + r)I_H, \quad (3)$$

$$\frac{dR_H}{dt} = rI_H - \mu_H R_H, \quad (4)$$

$$\frac{dS_M}{dt} = b_1(T)m_1(1 - \beta_w C) + b_2(T)m_2 - \beta_M(t)I_H S_M - \mu_M(T)S_M, \quad (5)$$

$$\frac{dE_M}{dt} = \beta_M(T)I_H S_M - (\mu_M(T) + \delta_M(T))E_M, \quad (6)$$

$$\frac{dI_M}{dt} = \delta_M(T)E_M + b_1(T)m_1\beta_w C - \mu_M(T)I_M, \quad (7)$$

$$\frac{dm_1}{dt} = \alpha\Lambda_M(T) - b_1(T)m_1 - Km_1^2 - \mu_1 m_1, \quad (8)$$

$$\frac{dm_2}{dt} = (1 - \alpha)\Lambda_M(T) - b_2(T)m_2 - \mu_2 m_2, \quad (9)$$

$$\frac{dC(t)}{dt} = \beta_0 I_H - \theta C. \quad (10)$$

The SEIR part of the model indicates that the population is divided into four categories: susceptible population (S_H), exposed population (E_H), infected population (I_H), and recovered population (R_H). In Equations (1)-(4), (T) denotes the temperature dependence function, and $\beta_H(T)$ represents the transmission rate of mosquitoes to humans. Specifically, $\beta_H(T) = b_m(T)\beta_{MH}(T)$, $b_m(T)$, where $b_m(T)$ is the bite rate and $\beta_{MH}(T)$ is the probability of mosquito infectivity. The term $\beta_H(T)\rho$ represents the rate of transmission from the infected

population to the susceptible population. μ_H is the natural mortality rate of humans, α_H is the rate at which the exposed population becomes infected, r is the rate of human recovery, and Λ_H is recruitment rate.

The SEI m_1m_2 part of the model describes the vector population, which is divided into adult and juvenile mosquitoes. The adult mosquito population N_M is divided into susceptible (S_M), exposed (E_M), and infected (I_M) populations. We further divided immature mosquitoes into two groups based on whether the water they were growing in was contaminated or not. Immature mosquitoes growing in polluted water are represented by m_1 , while those growing in unpolluted water are represented by m_2 . In Equations (5)-(9), $\Lambda_M(T)(>0)$ is recruitment rate, where $\Lambda_M(T) = N_F * \theta_M(T)$, N_F is the number of female mosquitoes, and $\theta_M(T)$ is the egg-laying rate of female mosquitoes. $\alpha\Lambda_M(T) (0 \leq \alpha \leq 1)$ is the recruitment rate of mosquitoes in polluted waters, and $\delta_M(T)$ is the probability of transitioning from E_M to I_M . $(1-\alpha)\Lambda_M$ is the recruitment rate of mosquitoes in unpolluted waters. $\beta_M(T)$ is the transmission rate from humans to mosquitoes, where $\beta_M(T) = b_m(T)\beta_{HM}(T)$, and β_{MH} is the mosquito infection probability. $b_i(T), i = 1, 2$ is the transformation rate from juvenile to adult mosquitoes, and $\mu_i, i = 1, 2$ is the mortality rate of juvenile mosquitoes. β_w denotes the infection rate of mosquitoes in contaminated water, $\mu_M(T)$ is the mortality rate of adult mosquitoes, and K is the density inhibition coefficient.

While C represents the average virus concentration in sewage, where β_0 is the scaling coefficient and θ represents the purification rate of virus concentration per unit time.

The SEIR-SEI $m_1m_2 - C$ flowchart mentioned above is shown in **Figure 1**.

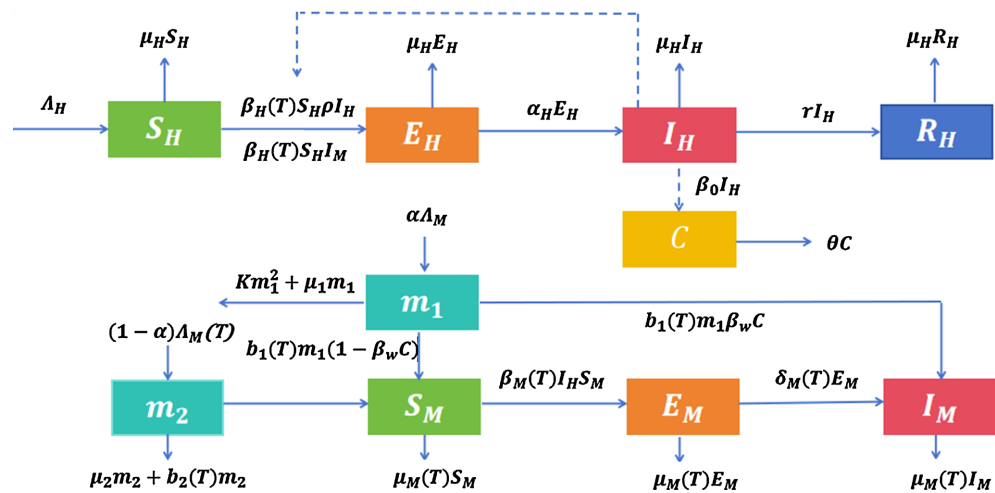


Figure 1. Flowchart of the Zika virus model.

2.2. The Basic Reproduction Number

One indicator that should not be ignored in infectious disease models is the basic reproduction number R_0 [15]. R_0 represents the average number of individuals one infected person will transmit the disease to before recovering. If $R_0 > 1$,

the epidemic will continue to spread. When $R_0 < 1$, the epidemic will disappear. In this paper, R_0 is the focus indicator.

The basic reproduction number R_0 can be calculated using the next-generation matrix method [15], which is:

$$R_0(T) = 2R_1(T) + R_2(T) + R_3(T),$$

where,

$$R_1(T) = \frac{\rho\beta_H(T)\Lambda_H\alpha_H}{2\mu_H k_1 k_2},$$

$$R_2(T) = \frac{\beta_0\beta_w\beta_H(T)\Lambda_H\alpha_H b_1 \bar{m}_1^*(T)}{\theta\mu_M(T)\mu_H k_1 k_2},$$

$$R_3(T) = \frac{\beta_M(T)\beta_H(T)\Lambda_H\alpha_H\delta_M(T)(b_1(T)\bar{m}_1^*(T) + b_2(T)\bar{m}_2^*(T))}{\mu_M(T)^2 \mu_H k_1 k_2 k_3(T)},$$

$$\bar{m}_1^*(T) = \frac{-(b_1(T) + \mu_1) + \sqrt{(b_1(T) + \mu_1)^2 + 4K\alpha\Lambda_M(T)}}{2K},$$

$$\bar{m}_2^*(T) = \frac{\Lambda_M(T)(1-\alpha)}{b_2(T) + \mu_2},$$

$$k_1 = \mu_H + \alpha_H, k_2 = \mu_H + r, k_3(T) = \delta_H + \mu_M(T).$$

2.3. Temperature-Dependent Parameters

Mosquitoes are crucial vectors in the transmission of the Zika virus (ZIKV). In the equations Equations (1)-(10), many parameters related to mosquitoes are temperature-dependent, such as the oviposition rate of female mosquito θ_M , recruitment rate (Λ_M), the survival probability of egg adult V_M , the probability of larva growing into adult b_i , the mortality rate of adult μ_M , the bite rate b_m , etc. In addition, parameters related to Zika virus transmission, such as the mosquito transmission probability (β_{MH}), mosquito infection probability (β_{HM}), and the conversion rate from E_M to I_M (δ_M), are also directly influenced by temperature. Use the method mentioned in [15] to establish a relationship with the temperature related parameters in Equations (1)-(10), as shown in **Table 1**. The Brière function takes the form $cT(T-T_0)(T_m-T)^2$, and the quadratic function takes the form $c(T-T_m)(T-T_0)$, where T denotes the temperature, T_0 denotes the minimum critical thermal temperature, and T_m denotes the maximum critical thermal temperature. c is the value of the parameter fitted by Mordecai *et al.* [14] through actual data.

According to the relationships listed in **Table 1**, a unimodal relationship between temperature and parameters θ_M , b_i , μ_M , β_M , β_H , δ_M is drawn. It can be seen from **Figure 2** that parameter β_H , β_M , δ_M , θ_M , b_i , μ_M^{-1} is the largest when the temperature reaches 31.6°C, 32.2°C, 37.8°C, 29.6°C, 28.9°C, 29.9°C respectively. The temperature ranges corresponding to the values of parameters β_H , β_M , δ_M and θ_M , b_i , μ_M^{-1} being greater than or equal to 0

Table 1. Thermal response matching life history characteristics of *Aedes aegypti*.

Trait	Definition	Function	Fitted Parameters		
b_m	Biting rate	Brière	$c = 2.02 \times 10^{-4}$	$T_{min} = 13.35$	$T_{max} = 40.08$
β_{MH}	The probability of mosquito infectivity	Brière	$c = 8.49 \times 10^{-4}$	$T_{min} = 17.05$	$T_{max} = 35.83$
β_H	The rate of mosquito transmission to humans	$b_m * \beta_{MH}$			
β_{HM}	The probability of mosquito infection	Brière	$c = 4.91 \times 10^{-4}$	$T_{min} = 12.22$	$T_{max} = 37.46$
β_M	Human and mosquito transmission rate	$b_m * \beta_{HM}$			
δ_M	The probability from E_M to I_M	Brière	$c = 6.65 \times 10^{-5}$	$T_{min} = 10.68$	$T_{max} = 45.90$
θ_M	Egg laying rate per female mosquito per day	Brière	$c = 8.56 \times 10^{-3}$	$T_{min} = 14.58$	$T_{max} = 34.61$
N_F	The number of female mosquitoes	N_F is a constant			
Λ_M	Recruitment rate	$\Lambda_M = \theta_M * N_F$			
Φ_M	Egg adult development rate	Brière	$c = 7.86 \times 10^{-5}$	$T_{min} = 11.36$	$T_{max} = 39.17$
V_M	Survival probability of egg adult	Quadratic	$c = -5.99 \times 10^{-3}$	$T_{min} = 13.56$	$T_{max} = 38.29$
b_i	The probability from m_i to S_M	$b_i = \Phi_M * V_M$			
μ_M^{-1}	Adult lifespan	Quadratic	$c = -1.48 \times 10^{-1}$	$T_{min} = 9.16$	$T_{max} = 37.73$

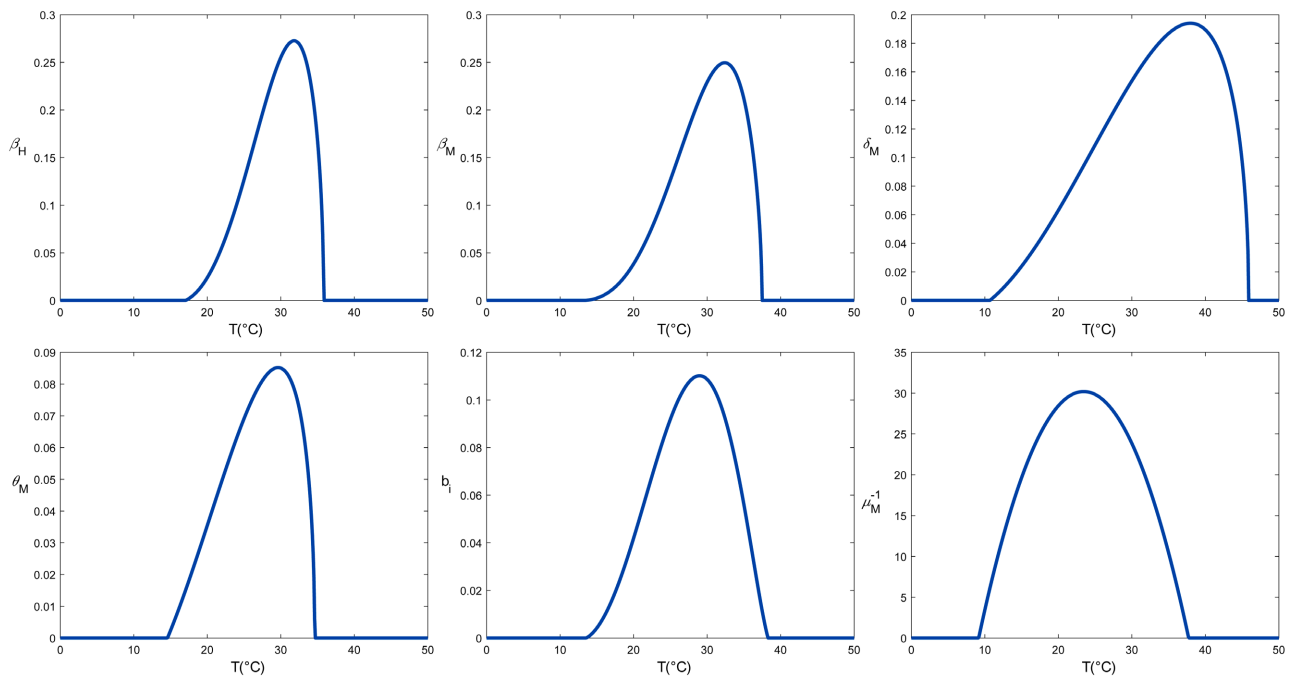


Figure 2. The effect of temperature on parameters.

are $T \in [17.1^\circ\text{C}, 36.2^\circ\text{C}]$, $T \in [13.9^\circ\text{C}, 37.4^\circ\text{C}]$, $T \in [10.8^\circ\text{C}, 45.9^\circ\text{C}]$,
 $T \in [14.5^\circ\text{C}, 34.7^\circ\text{C}]$, $T \in [13.5^\circ\text{C}, 38.9^\circ\text{C}]$, $T \in [14.5^\circ\text{C}, 34.7^\circ\text{C}]$, respectively.

2.4. Estimation of Parameter Values in the Model

The natural mortality rate of human beings is set at $\mu_H = 0.00004$ with reference

to the relevant literature [16]. The average recovery rate for Zika virus is set at $r = 0.5$ according to [17]. According to [13], the sewage purification rate is set at $\theta = 0.84$. Considering that the average annual temperature in Brazil is $T = 24^\circ\text{C}$ [18], substituting this temperature into **Table 1** yields the following values for the corresponding parameters: $\theta_M = 0.063$, $b_i = 0.083$, $\mu_M = 0.0332$, $\beta_M = 0.1054$, $\beta_H = 0.1008$, and $\delta_M = 0.0995$. To estimate the remaining fixed parameter values in the model described by Equations (1)-(9), we fitted the parameters using the least squares method. The data used were the weekly number of suspected Zika virus infections from April 4, 2015, to December 4, 2015 [19]. Not only that, we also obtained the population data of Brazil in 2015 from the Brazilian census in 2015 for the approximate determination of the initial population range [20].

Assuming that the cumulative number of new infections per week is recorded as $P(t)$, then $P(t)$ satisfies the following expression:

$$\frac{dP}{dt} = \eta\alpha_H E_H,$$

where η represents the proportion of reported cases. The data we fit starts from April 4, 2015. Therefore, we set $P(0)$, representing the number of new infections in Brazil on March 28, 2015, to 7343.

2.5. Seasonal Forcing

The temperature fluctuation curve indicates a certain periodicity, hence we introduce a seasonal component. Observations reveal that the annual temperature in Brazil exhibits a trend of being higher at both ends of the year and lower in the middle. Consequently, we model the temperature as a function of time, establishing a cosine curve with a period of 365 days, as shown below,

$$T(t) = \frac{T_{max} - T_{min}}{2} * \left(-\cos\left(\frac{2\pi}{365}(t - \omega)\right) \right) + T_{mean}. \quad (11)$$

where T is the temperature (in degrees Celsius) and (t) is the time in days, T_{max} , T_{mean} and T_{min} represent the annual maximum, mean, and minimum temperatures, respectively. ω is the phase shift that aligns the sinusoidal function with the seasonal factors of each Brazilian city. We combined Equations (1)-(9), Equation (2) with the actual temperatures of the Brazilian cities as a way to analyze the effect of seasonal variations on the propagation of Zika virus in different cities of the Brazilian region.

2.6. Removal of Data Outliers

In this paper, boxplot method is used to detect outliers. Boxplot was invented in 1977 by John Tukey, an American statistician, which shows the characteristics of the actual data and visually identifies outliers in the data batch [21]. To construct a boxplot, it is essential to determine the maximum value, minimum value, median, and the lower (Q_1) and upper quartiles (Q_3) of the data. The difference

between the upper and lower quartiles is referred to as the interquartile range (*IQR*). Outliers are defined as data points that fall outside the range of $(Q_1 + 1.5IQR, Q_3 - 1.5IQR)$. As an example, the daily high temperature data of Porto Alegre from January 1, 2015, to January 1, 2023, and from January 5, 2015, to January 5, 2023, are used to plot the corresponding box plots, as shown in **Figure 3**. As can be seen from **Figure 3**, there is no abnormal temperature on January 1, 2015-2023, while there is an abnormal temperature on January 5, 2015-2023 that needs to be removed.

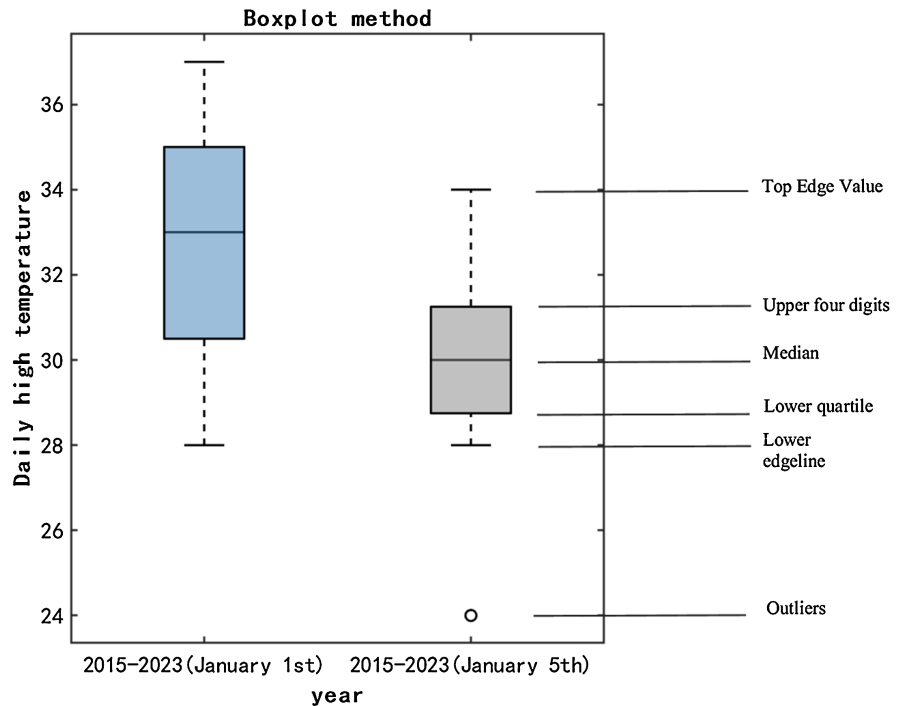


Figure 3. High temperature data processing from January 1, 2015 to 2023 and January 5, 2015 to 2023 in Porto Alegre (Boxplot method).

2.7. Sensitivity Analysis

In order to examine the sensitivity of the control parameters to the basic reproduction number, this paper uses the normalized forward sensitivity index method [22]. Mathematically, the sensitivity index (*SI*) of R_0 with respect to parameter p is defined as:

$$r_p^{R_0} := \frac{\partial R_0}{\partial p} \times \frac{p}{R_0}.$$

The sensitivity index can be either positive or negative. A positive sensitivity index indicates that the basic reproduction number increases as the parameter increases, whereas a negative sensitivity index indicates that the basic reproduction number decreases as the parameter increases. In addition, to assess the reliability and robustness of the model, we used the partial rank correlation coefficient (PRCC) method [23] to determine the effect of changes in the parameters identified by the

fit calibration on the basic reproduction number of the model. The PRCC provides a quantitative assessment of the impact of each parameter on the model output. The sign and magnitude of the PRCC indicate the direction and strength of the effect of each parameter on the output variables. Positive PRCC values suggest that an increase in the parameter results in an increase in the basic reproduction number, while negative PRCC values suggest that an increase in the parameter results in a decrease in the basic reproduction number. A larger absolute value of PRCC represents a more significant effect. Additionally, we used the Latin hypercube sampling method to generate 10000 random samples for each parameter. These samples cover the range of possible parameter values.

3. Data

3.1. Historical Weather Data

Because the Zika virus outbreak in Brazil started since 2015, this paper uses data from 2015-2023 as a historical baseline. Historical daily low and daily high temperatures for 9 years (2015-2023) were compiled from [24]. From this, the average daily temperature, the annual maximum temperature, the average annual temperature, and the annual minimum temperature were obtained for the calendar years 2015-2023. The corresponding ω values for each city were obtained by least squares fitting of the obtained data with Equation (11).

3.2. Future weather data

World Climate Research Programme (WCRP) Working Group on Coupled Modelling (WGCM) collects and compares simulation results from various global climate models through Coupled Model Intercomparison Project (CMIP). According to statistics, in 2016 alone, climate-related articles published in the Journal of Climate that explicitly cited CMIP5 accounted for 45% of all articles [25]. This is a great indication that CMIP plays an extremely important role in climate research. WCRP organized CMIP6 [24] refcmip6.1, refcmip6.2, refcmip6.3, refcmip6.4, and the number of models participating in CMIP6 this time increased significantly compared with the past. Only the model development team participating in CMIP6 increased by 13 institutions compared with CMIP5, and the model of CMIP6 increased by more than 70 to 112 compared with the more than 40 model versions of CMIP5. With the information [24] ref6.41, ref6.42, it is clear that GFDL-ESM4 [24] ref6.5 is the most accurate model for capturing historical temperatures in South America in the CMIP6 model. Therefore, the GFDL-ESM4 model was selected in this paper to obtain historical and predicted future temperature data. The relevant files were downloaded from the public website [24] refhttp, and by looking at the file information, it is known that the resolution (number of meridional grids \times number of latitudinal grids) of the GFDL-ESM4 model is 288×180 , which means that the grid resolution of GFDL-ESM4 is $1^\circ \times 1.25^\circ$. In order to extract the relevant data of the required ten cities, we use nearest neighbor interpolation to process the grid resolution of the data to $0.5^\circ \times 0.5^\circ$, and

then extract the nearest model grid point to each city, which represents the city.

In the projections, the years 2060–2070 were selected as the projection years. Four Shared Socioeconomic Pathways (SSP) climate scenarios were used: SSP126, SSP245, SSP370 and SSP585 [24] refssp. These scenarios represent different levels of climate-related socioeconomic development and their corresponding GHG concentrations. SSP126 is a low-emission scenario that requires significant global efforts and government intervention to achieve. In contrast, SSP585 is a high-emission, baseline scenario characterized by increasing greenhouse gas emissions and concentrations, with no climate change intervention. SSP245 and SSP370 fall between these two extremes, suggesting that future societies can partially adapt.

4. Results

4.1. Data Fitting

Table 2 presents the parameter values calibrated through data fitting, with the fitting results being statistically significant as indicated by the p-values [26]. We substituted these fitting results into Equation (1) and compared the predicted results with the actual results (as shown in **Figure 4**), finding a good agreement between them.

Table 2. Parameter values for Brazil region data fitting calibration.

Parameter	Parameter value	Standard error	Confidence interval	p-value
K	0.000010249	3.34E-06	[3.3186e-6, 0.00001718]	0.0056449
α	0.756631	0.196735	[0.348628, 1.164635]	0.775284E-4
α_H	0.00848635	0.00165192	[0.005060478, 0.0119122]	0.7808999E-5
β_0	1.9637	0.00020044	[1.9633, 1.9641]	0.5436e-5
β_w	0.018233	0.0001472	[0.017928, 0.018538]	0.7244e-3
η	0.00522087	7.592665E-4	[0.00364625, 0.00679549]	0.614422E-7
ρ	0.59029	0.0026858	[0.58472, 0.59586]	0.927e-38
μ_1	0.910935	0.368895	[0.1458932, 1.675978]	0.021773
μ_2	0.870216	0.296051	[0.2562443, 1.484187]	0.007586

It is crucial to consider the robustness and reliability of the model, acknowledging that environmental changes or specific geographical factors may cause some of the fitted parameters to vary within a certain range. We employed PRCC quantitative analysis to assess the impact of the parameter values obtained from model fitting on the basic reproduction number of the model. As illustrated in **Figure 5**, none of the parameters are sensitive to R_0 , except for parameters μ_1 and μ_2 . According to [27], the mortality rate μ_2 ranges from 0.8 to 0.9, and our fitting results fall within this range. Despite our inability to find relevant

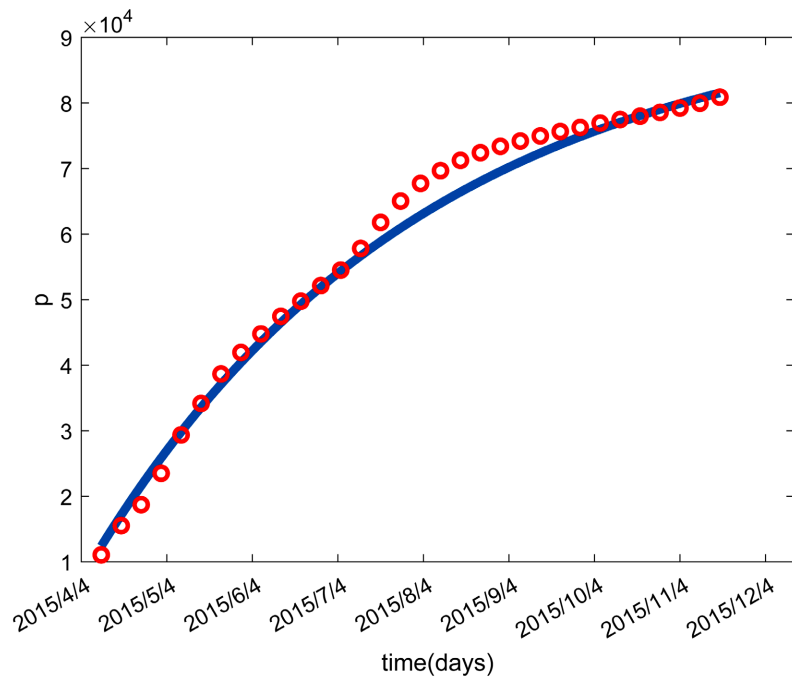


Figure 4. The fit of p :graph comparing predicted infection data with actual infection data.

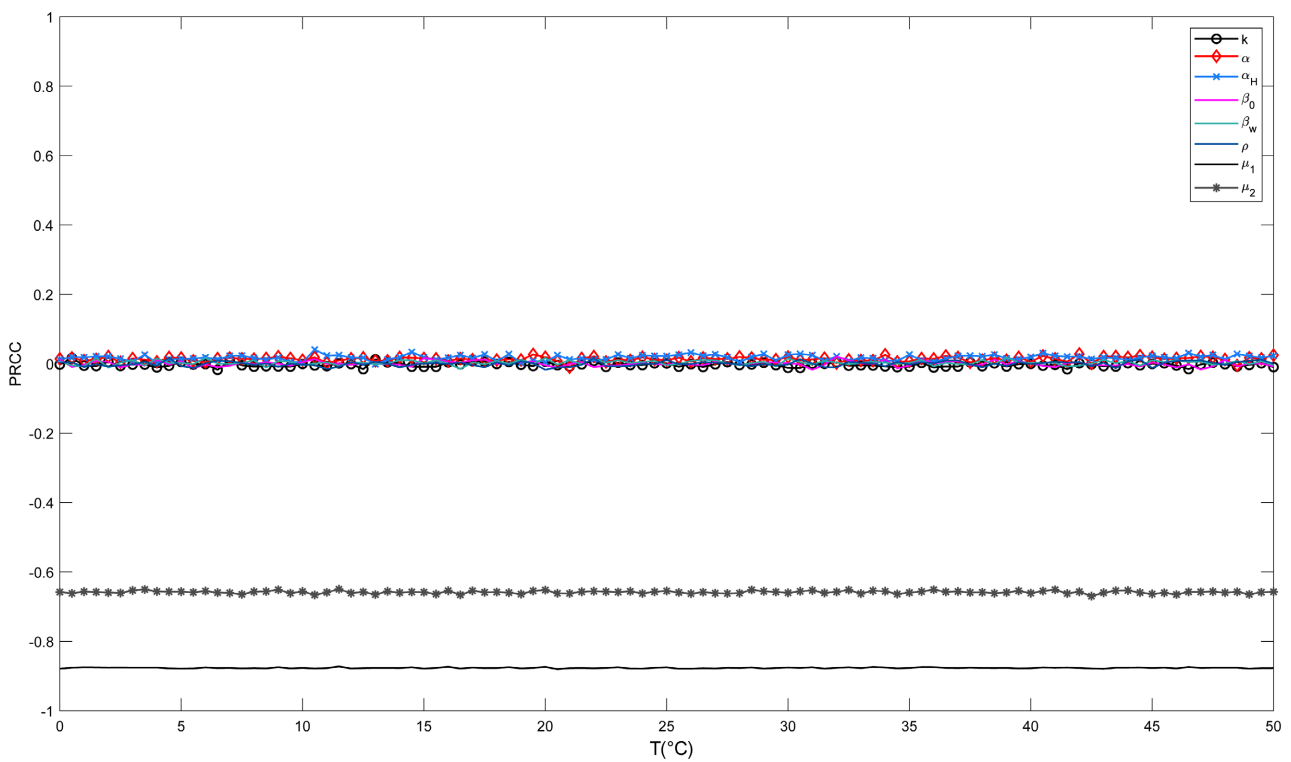


Figure 5. Effect of fitting parameters on R_0 at different temperatures.

literature on mosquito mortality in polluted waters, our assumption that mosquitoes in polluted water bodies are subject to density control, which increases mosquito mortality, makes the fitting results reasonable to some extent. Consequently,

appropriate parameter changes are not expected to significantly impact the predicted results of the model, thereby confirming the model's reliability.

4.2. Effect of Temperature on Zika Virus Spreading

From **Figure 6**, it can be seen that there is a single-peak relationship between temperature and the basic reproduction number, with R_0 peaking at 3.2, which corresponds to a temperature of about 29.4°C. The temperature range where $R_0 > 1$ is $T_x \in (23.34^\circ\text{C}, 33.99^\circ\text{C})$.

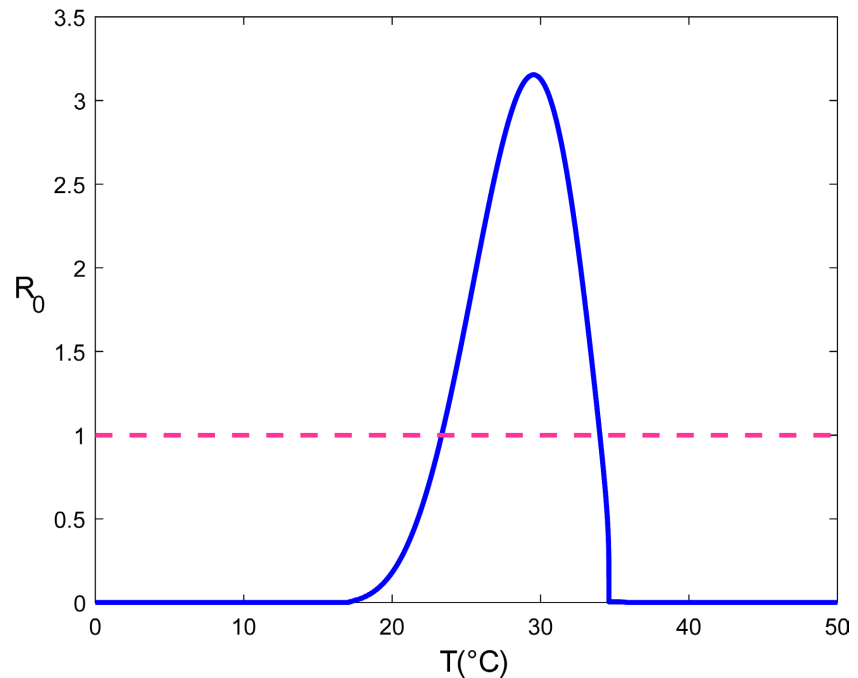


Figure 6. The effect of temperature T on R_0 .

From **Figure 7**, it can be seen that when the temperature is between 18°C and 35°C, the final number of infected people remains greater than zero. At other temperatures, the final number of infected people tends to zero.

4.3. Impact of Seasonal Variations on Zika Virus Transmission in the Brazilian Region

In order to study the potential impact of seasonal variations on different cities in the Brazilian region, a total of ten important Brazilian cities were selected for analysis: Manaus, Palmas, Macapa, Rio de Janeiro, Teresina, Recife, Aracaju, Sao Paulo, Porto Alegre, and Florianópolis.

4.3.1. Analysis of Basic Reproduction Numbers in Different Regions Based on Historical Temperatures

Based on the methodology described in Section 3, the values of T_{max} , T_{mean} , T_{min} and ω were calculated for the 10 cities over the period from 2015 to 2023 and substituted into Equation (11). This enabled us to obtain the temperature as a

function of time for different years in each city, and consequently, the basic reproduction number under the influence of temperature exhibited a corresponding change. Taking Porto Alegre as an example, **Figure 8** illustrates the city's temperature variation for each year from 2015 to 2023, while **Figure 9** depicts the corresponding

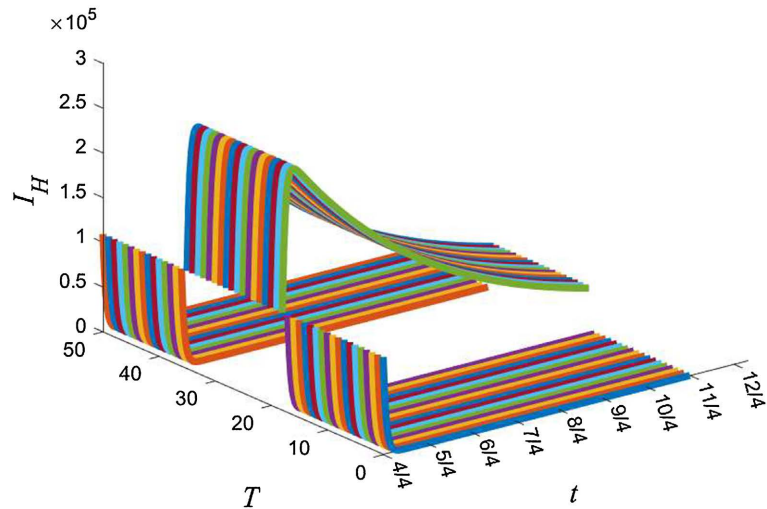


Figure 7. The effect of temperature T on I_H .

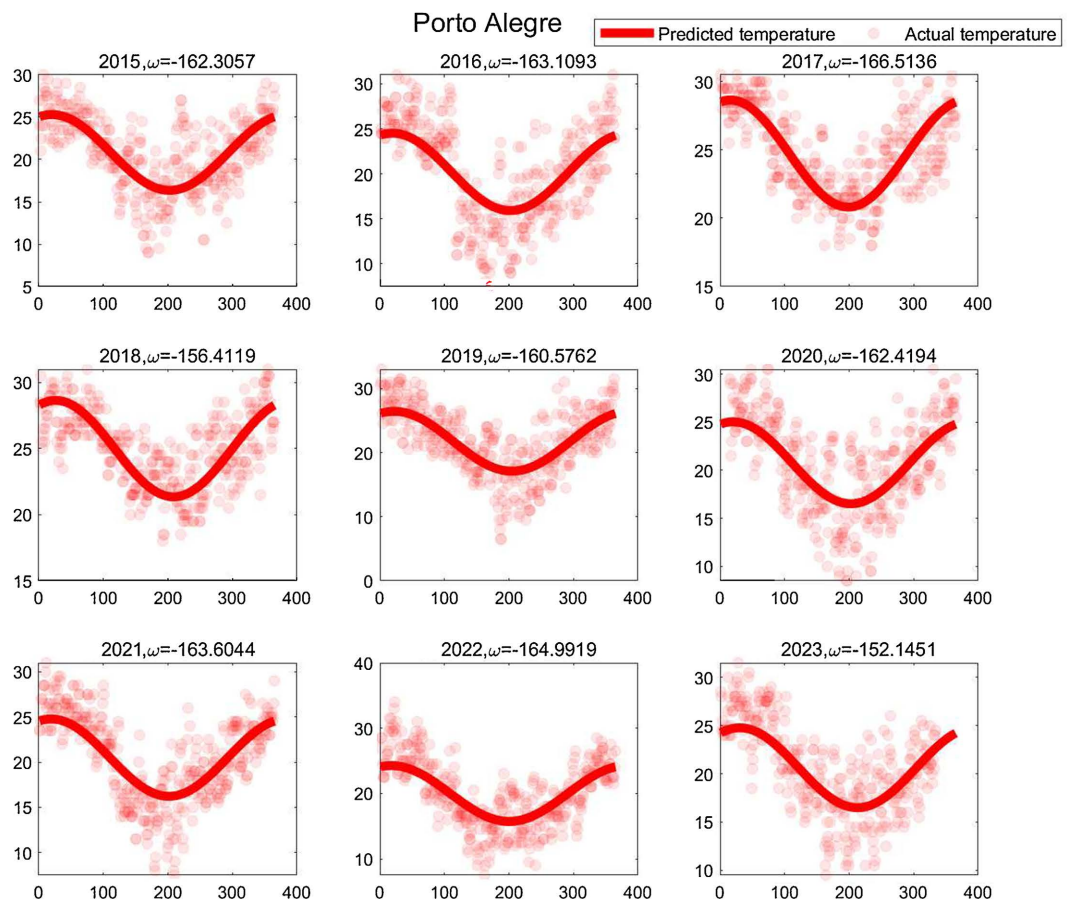


Figure 8. Daily temperature versus fitted seasonal temperature profile in Porto Alegre, 2015-2023.

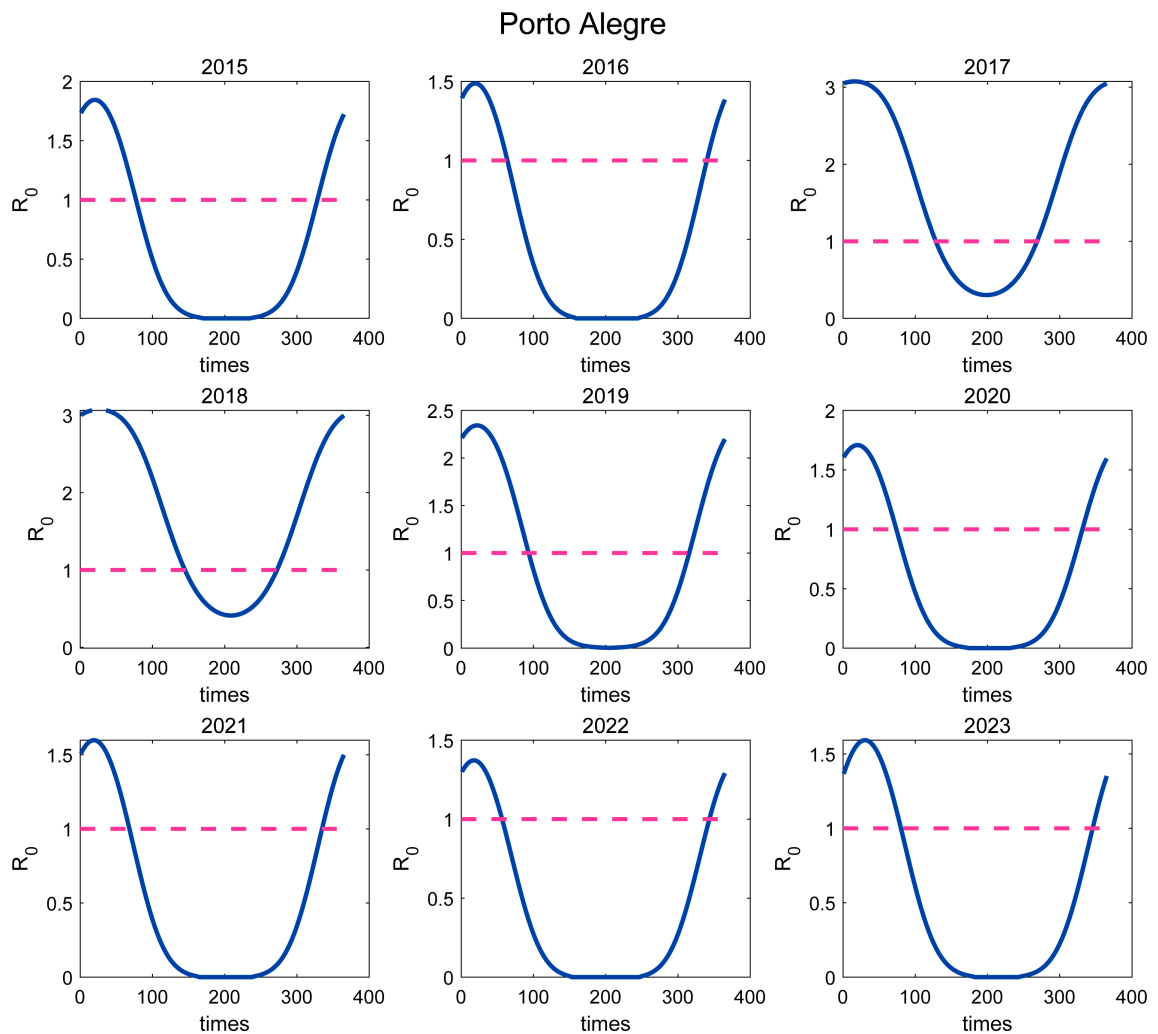


Figure 9. Daily change in basic reproduction number in Porto Alegre, 2015-2023.

variation in the basic reproduction number. Therefore, the dates that require attention for Zika virus prevention and control vary from year to year, as can be seen from **Figure 9**, in 2015, Porto Alegre focused on the prevention and control of Zika virus during the periods of January 1, 2015 to March 19, 2015 and November 26, 2015 to December 31, 2015, respectively. Whereas in 2018, the dates that needed to be focused on the prevention and control of Zika virus were during the period from January 1, 2018 to May 25, 2018 and from October 1, 2018 to December 31, 2018, which is almost the whole year.

Next, consideration was given to extracting commonalities from these nine years of data to generate a new dataset, which could be used to construct a basic reproduction number model that can represent the period from 2015 to 2023. However, it is not reasonable to represent the data as a mean only, as the daily mean temperature is not constant across the years and there are likely to be extremes in a given year. It is important that such extremes are detected and dealt with when analyzing the data to avoid biasing the results of the analysis [28].

Using the boxplot methodology mentioned in Section 2, outliers were removed,

and a model of the historical annual mean temperature change in the same city was constructed based on the mean values. This, in turn, yielded a model of the change in the basic reproduction number. Using Porto Alegre as an example, we plotted the seasonal temperature variation and the corresponding average annual trend of the basic reproduction number (see **Figure 10**, **Figure 11**). The model is

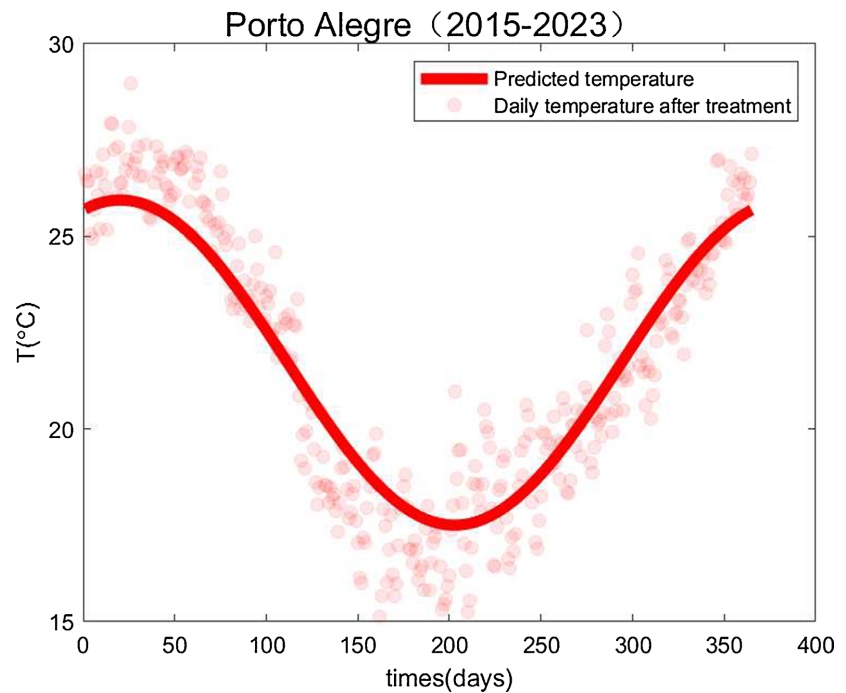


Figure 10. Temperature modeling in Porto Alegre, 2015-2023.

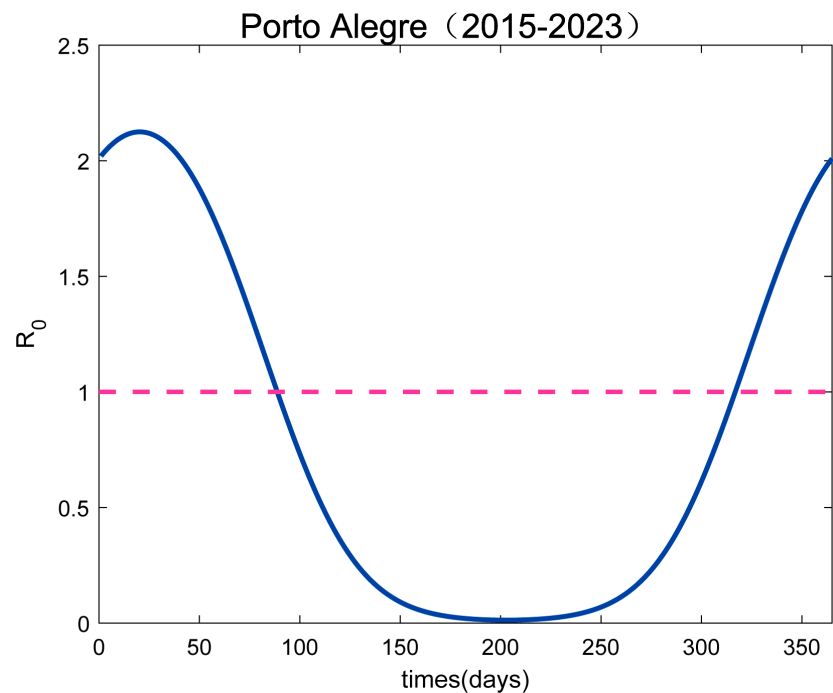


Figure 11. The basic reproduction number model for Porto Alegre, 2015-2023.

a risk estimation model based on historical temperatures, which allows us to estimate the risk of Zika virus at current temperatures, determine the approximate basic reproduction number, and identify the approximate time periods for which Zika virus prevention and control are needed.

By comparison, we find that some of these ten regions have similar temperature variations, while others are quite different. Therefore, the ten regions are categorized according to the type of climate [29] and the average annual temperature: 1) Tropical Rainforest Climate Cities: exemplified by Manaus, Palmas, and Macapa, all with an average daily temperature of around 27°C. 2) Tropical Savanna Climate Cities: exemplified by Rio de Janeiro. 3) Tropical Climate Cities: exemplified by Teresina. 4) Cities with Tropical Monsoon Climate: exemplified by Recife and Aracaju. 5) Subtropical Climate Cities: exemplified by Sao Paulo, Porto Alegre, and Florianópolis. The following analysis focuses on these five climate types of cities. To integrate the data for cities within the same category, the box plot method was used to identify outliers in the average daily temperatures of different cities on the same date. These outliers were then removed, and the remaining data were averaged.

This results in a temperature model and a basic reproduction number model that can represent the cities of these five climate types, as shown in **Figure 12**, **Figure 13**. From **Figure 12**, it can be seen that the temperatures of the cities of

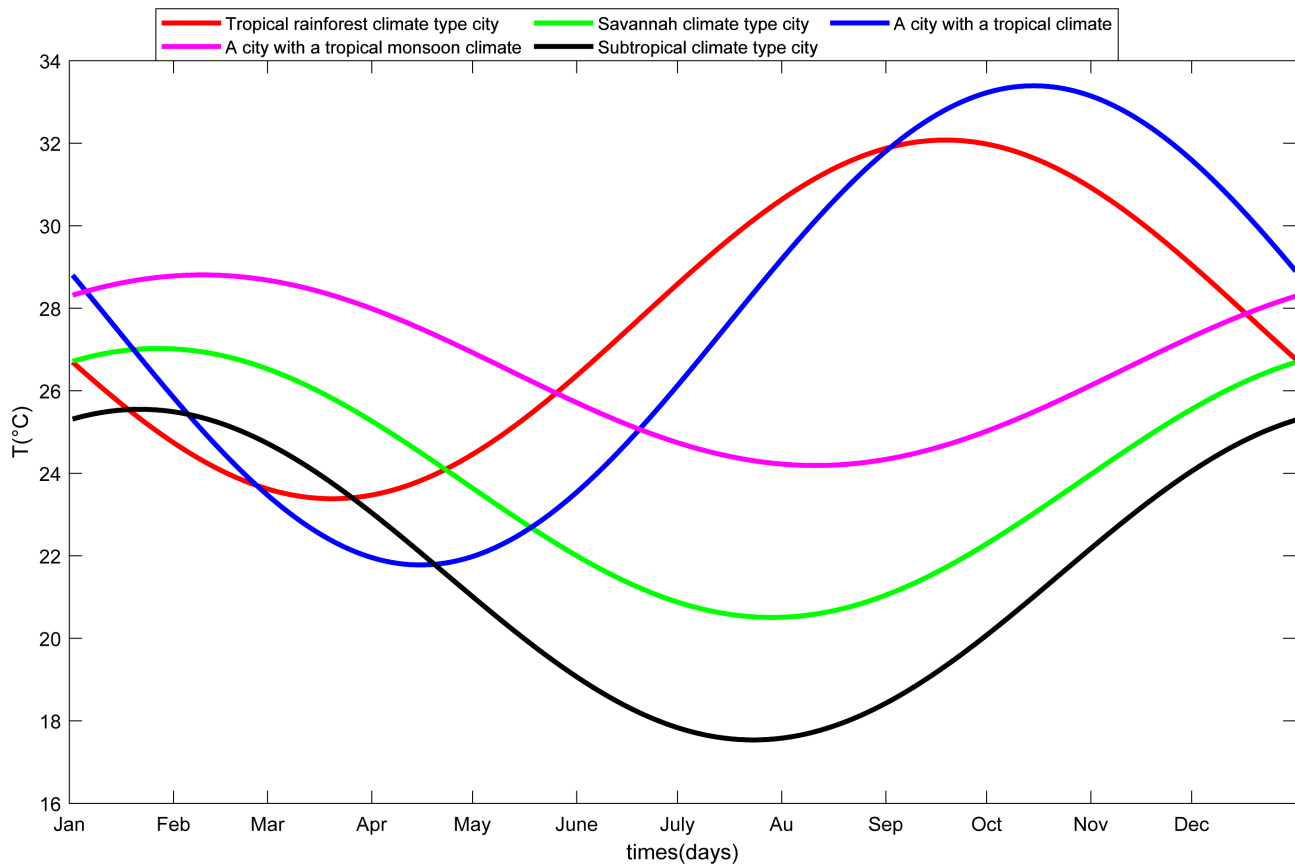


Figure 12. Daily changes in urban temperatures for five climate types, 2015-2023.

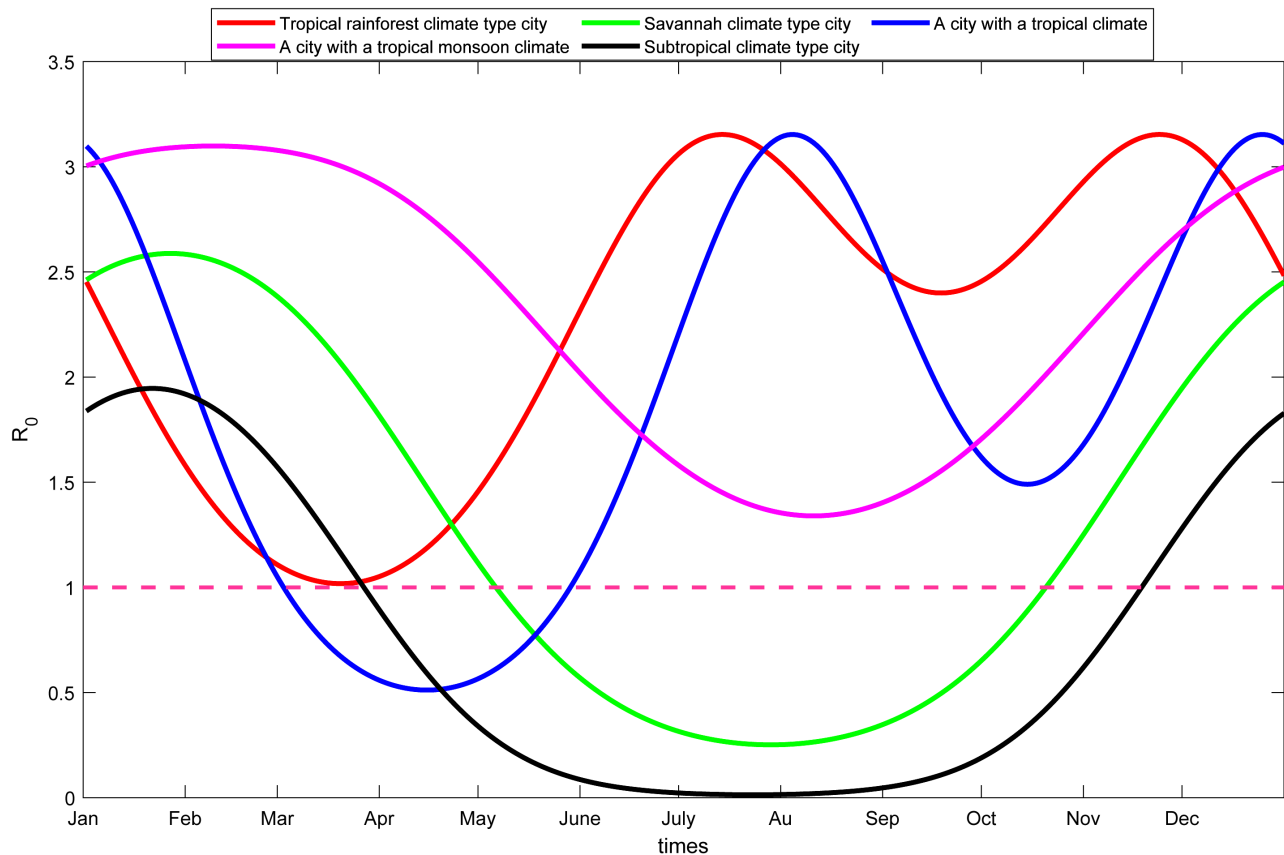


Figure 13. Daily changes in the basic reproduction number in cities for five climate types, 2015-2023.

different climate types in the Brazilian region vary considerably, which leads to a large difference in the corresponding basic reproduction number models. From **Figure 13**, it can be seen that cities with Tropical Rainforest Climate and Tropical Monsoon Climate have $R_0 > 1$ almost year-round. This suggests that the government needs to focus on the prevention and control of Zika virus throughout the year in these two types of cities. In cities with a Tropical Savanna Climate, the time periods requiring Zika virus control are from January 1 to May 5 and from October 20 to December 31. In Subtropical Climate type cities, the time period for Zika virus prevention and control are from January 1 to March 26 and from November 18 to December 31.

4.3.2. Risk Prediction for Zika Virus Based on Future Temperature Data

In Section 3, we obtained temperature projections for ten regions in Brazil for 2060-2070 under different scenarios. These data can be used to project changes in Zika virus risk for cities with different climate types under various SSP climate scenarios. We plotted the trends in temperature and the basic reproduction number for five climate type cities under different SSP climate scenarios, as shown in **Figures 14-18**. From these plots, it can be seen that there are differences in the risk of Zika virus under different SSP climate scenarios. When the future is under the SSP126 climate scenario, the risk of Zika virus is smaller compared to the

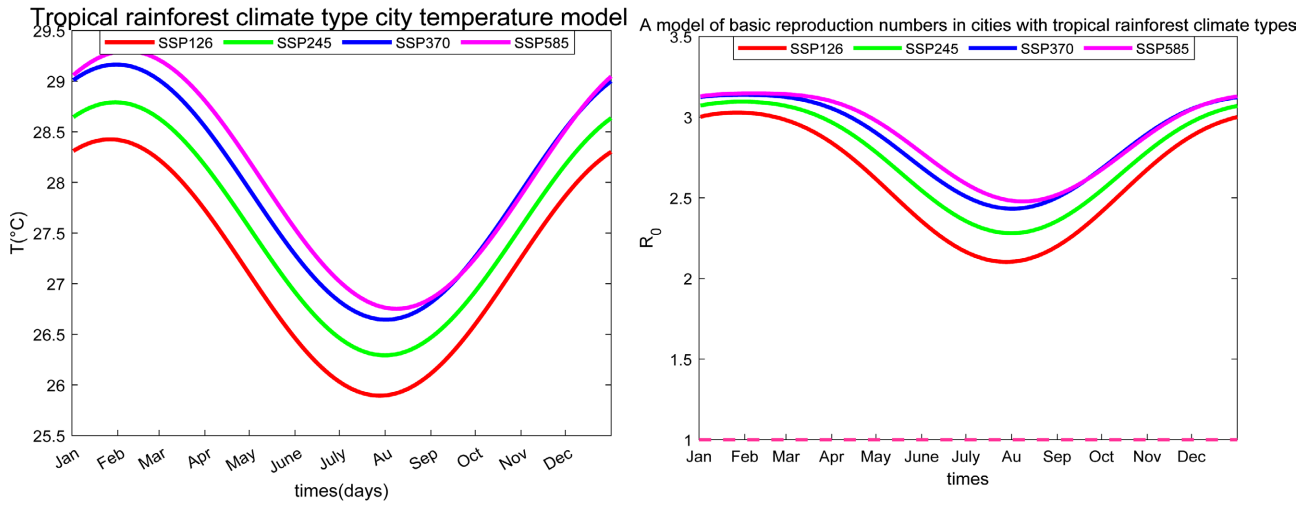


Figure 14. Modeling Temperature and Basic Reproduction Numbers for Cities with Tropical Rainforest Climate Types, 2060-2070.

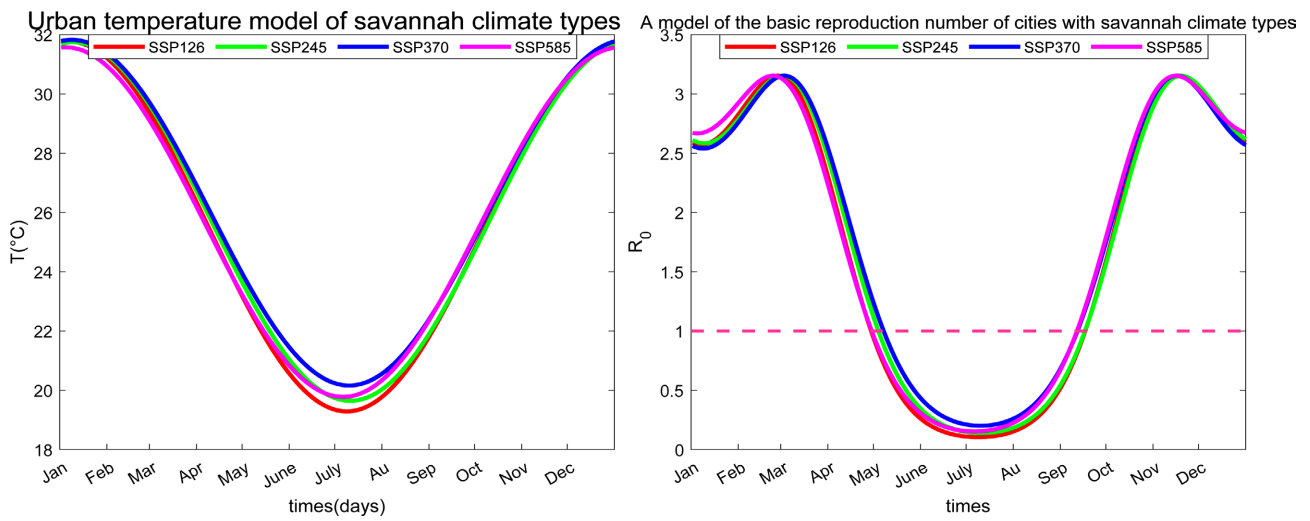


Figure 15. Modeling Temperature and Basic Reproduction Numbers for Cities in the Tropical Savanna Climate Type, 2060-2070.

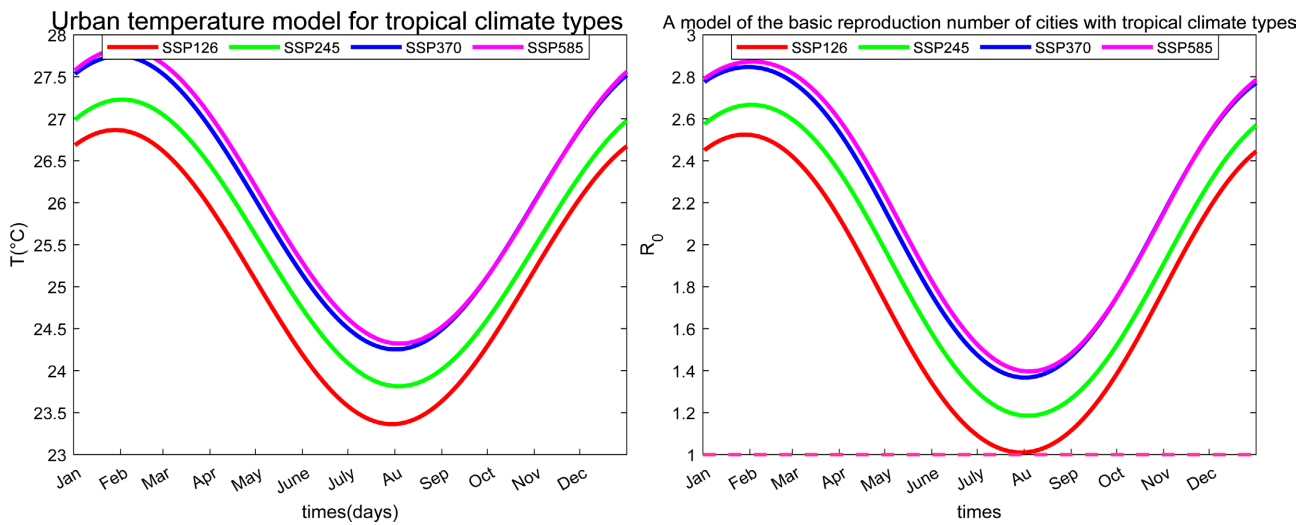


Figure 16. Modeling Temperature and Basic Reproduction Numbers for Cities with Tropical Climate Types in 2060-2070.

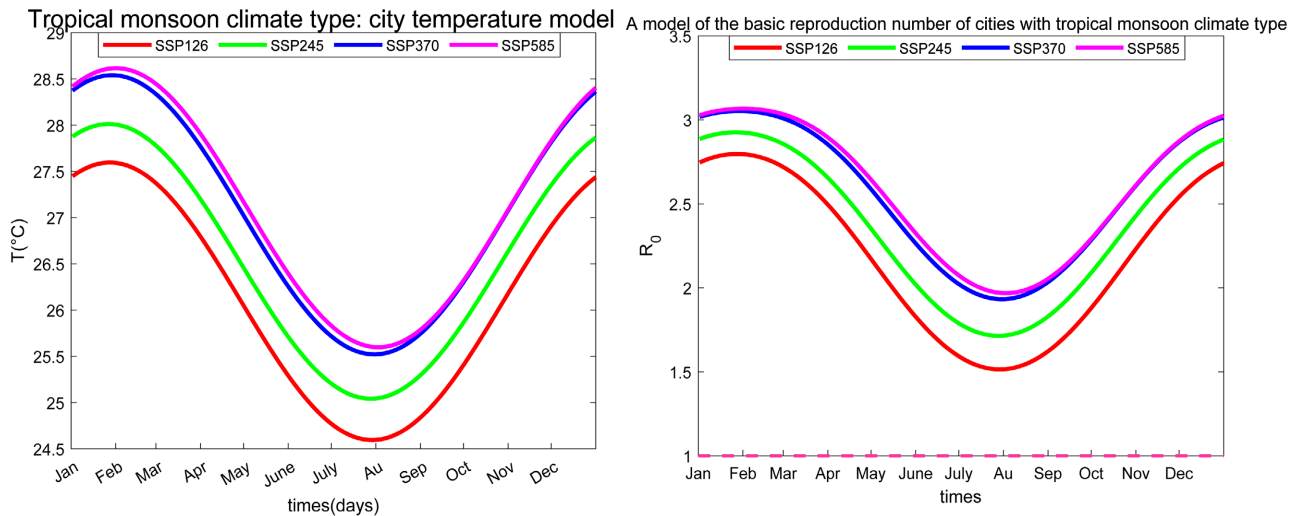


Figure 17. Temperature and basic reproduction number modeling for cities with tropical monsson climate types, 2060-2070.

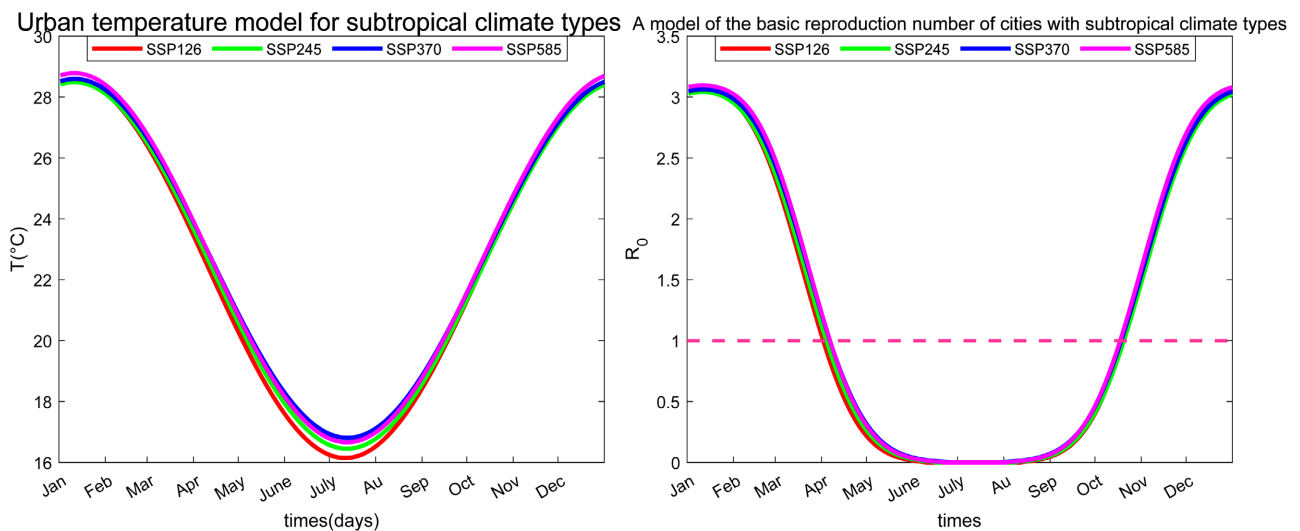


Figure 18. Temperature and basic reproduction number modeling for Subtropical Climate Climate type cities in 2060-2070.

SS585 climate scenario. However, regardless of the scenario, the time in the future when Zika virus needs to be prevented and controlled will expand. In particular, the areas covered by the tropical rainforest climate zone, the tropical climate zone, and the tropical monsoon climate zone are risk zones throughout the year.

Using the above five climate types as a proxy and extending the projections to the entire Brazilian region, we have mapped the Zika virus risk projections for Brazil for different months based on the future temperatures projected by SSP126 for the years 2060-2070. As shown in Figure 19, the months with the highest prevalence of Zika virus in Brazil will be from August to December. Additionally, we found that the northwestern region of Brazil will be in the Zika virus early warning stage almost all year round, indicating that authorities should focus their Zika virus prevention and control efforts on these areas. This is because Zika virus may be more likely to cause an outbreak after a long period of accumulation.

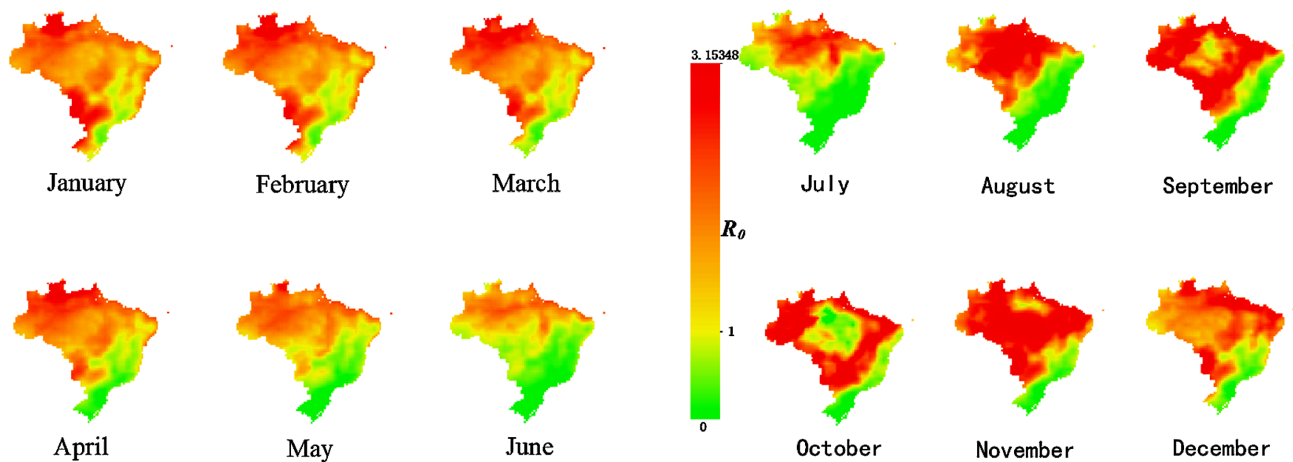


Figure 19. Zika virus risk forecasting map of Brazil.

4.4. Control Strategies of Zika Virus under the Influence of Temperature

This section discusses the sensitivity of control parameters to the basic reproduction number from a control perspective and provides a reference for the selection and implementation of control measures. Commonly used control measures include: 1) Reducing the values of parameters β_H and β_M by installing anti-mosquito screens, using mosquito nets, and other similar measures. 2) Increasing the values of parameters μ_M and μ_i through the use of insecticides and other interventions. 3) Maintaining the cleanliness of the water environment to reduce the values of parameters α and β_0 . 4) Reduce the mosquito population (N_F) using the Sterile Insect Technique (SIT).

The sensitivity index of R_0 to each model control parameter at different temperatures are shown in Figure 20. Two different sensitivity analyses were used: the normalized forward sensitivity index and PRCC, presented in Figure 20(a) and Figure 20(b), respectively. From Figure 20(a), Figure 20(b), it can be seen that α, β_0 are insensitive to R_0 when the temperature $T \in (17^\circ\text{C}, 36^\circ\text{C})$. This is also confirmed by Figure 20(c) and Figure 20(d), where changes in the values of α and β_0 are barely able to make $R_0 < 1$. On the other hand, μ_M exhibits the highest sensitivity to R_0 . As shown in Figure 20(h), increasing the value of μ_M to a critical level can reduce R_0 below 1. Additionally, N_F, β_H and β_M are also sensitive to R_0 . This we can also see in Figures 20(e)-(i). Particularly when $T \in (35^\circ\text{C}, 35.5^\circ\text{C})$, the sensitivity index of β_H to R_0 reaches 1 at one point. This suggests that it is crucial to focus on using mosquito nets, repellents, and similar measures to reduce mosquito bites when the temperature is around $(35^\circ\text{C}, 35.5^\circ\text{C})$. In daily life, we often observe synergistic control through these measures. For instance, efforts to prevent mosquito bites simultaneously reduce both mosquito-to-human virus transmission (β_H) and human-to-mosquito transmission (β_M). Figure 21 illustrates the effect on R_0 when β_H and β_M are simultaneously reduced. Meanwhile, we can see from Figure 20(g), Figure 20(h) that the adult mosquito mortality rate (μ_M), the larvae mortality rate (μ_i)

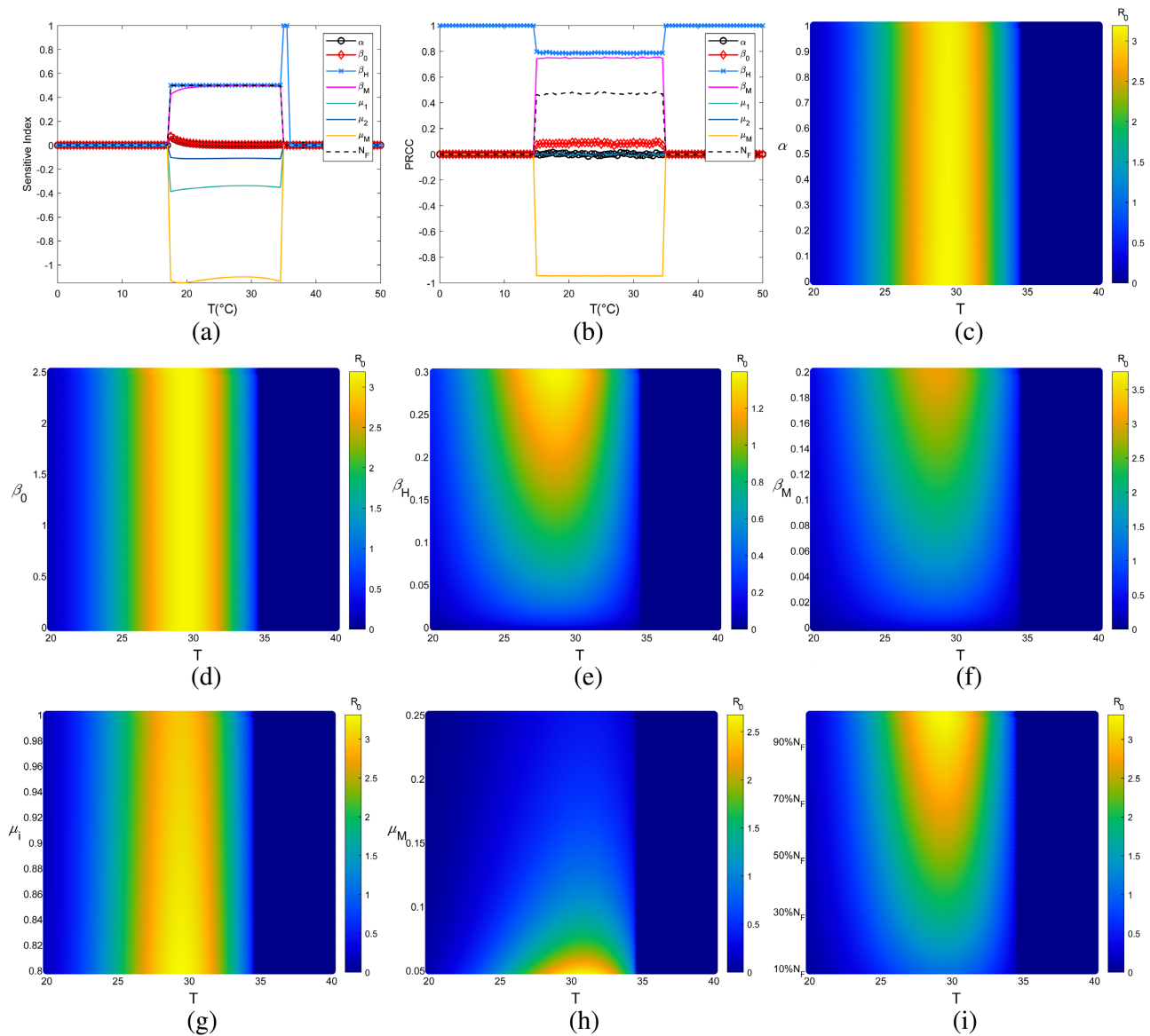


Figure 20. Influence of temperature and control parameters on R_0 .

cannot be ignored. In addition, we we focused on the use of insecticides and mosquito lamps to increase the adult mosquito mortality rate (μ_M), and the use of earthy yellow sand to fill various pits, depressions, ditches, and other places where water tends to accumulate to increase the larvae mortality rate (μ_i). From **Figure 22(a)**, it can be seen that $R_0 < 1$ can be achieved when μ_M and μ_i reach a specific range. From **Figure 22(b)**, it is evident that in their synergistic control, controlling the adult mosquito mortality rate (μ_M) is crucial. For example, at $T = 30^\circ\text{C}$ and $T = 32^\circ\text{C}$, the adult mortality rate (μ_M) must be greater than 0.11 to control the outbreak of the Zika virus(as shown in **Figure 22(c)**, **Figure 22(d)**). This means that at this point, the life span of adult mosquitoes to be controlled does not exceed an average of about 9 days.

In addition to the conventional control methods mentioned above, SIT offers a

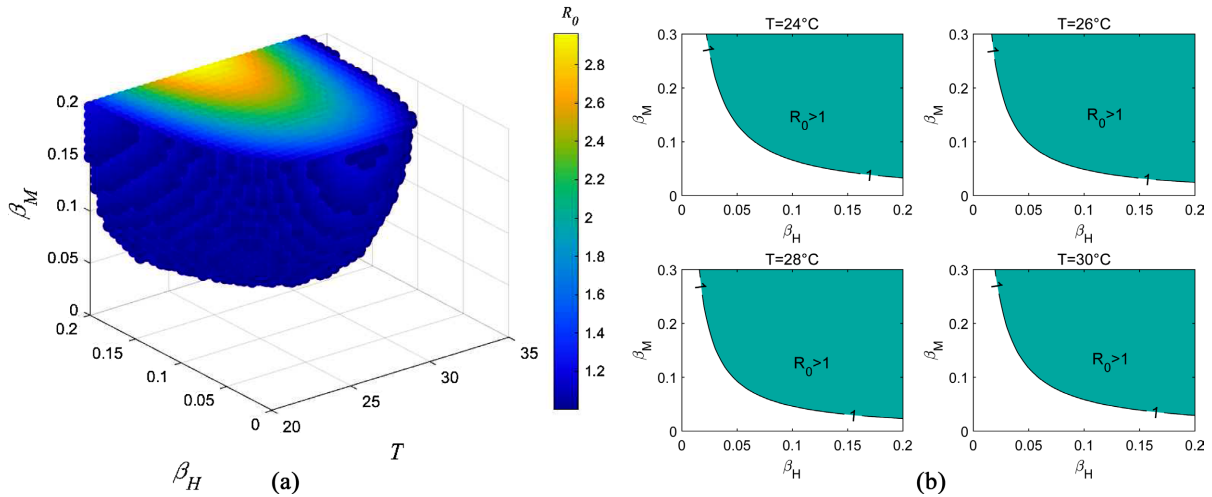


Figure 21. Temperature and β_H , β_M together on R_0 . (a) where the white part indicates that $R_0 < 1$ when (b) The green part indicates $R_0 > 1$ and the white part indicates $R_0 < 1$. colored part indicates the case where $R_0 > 1$.

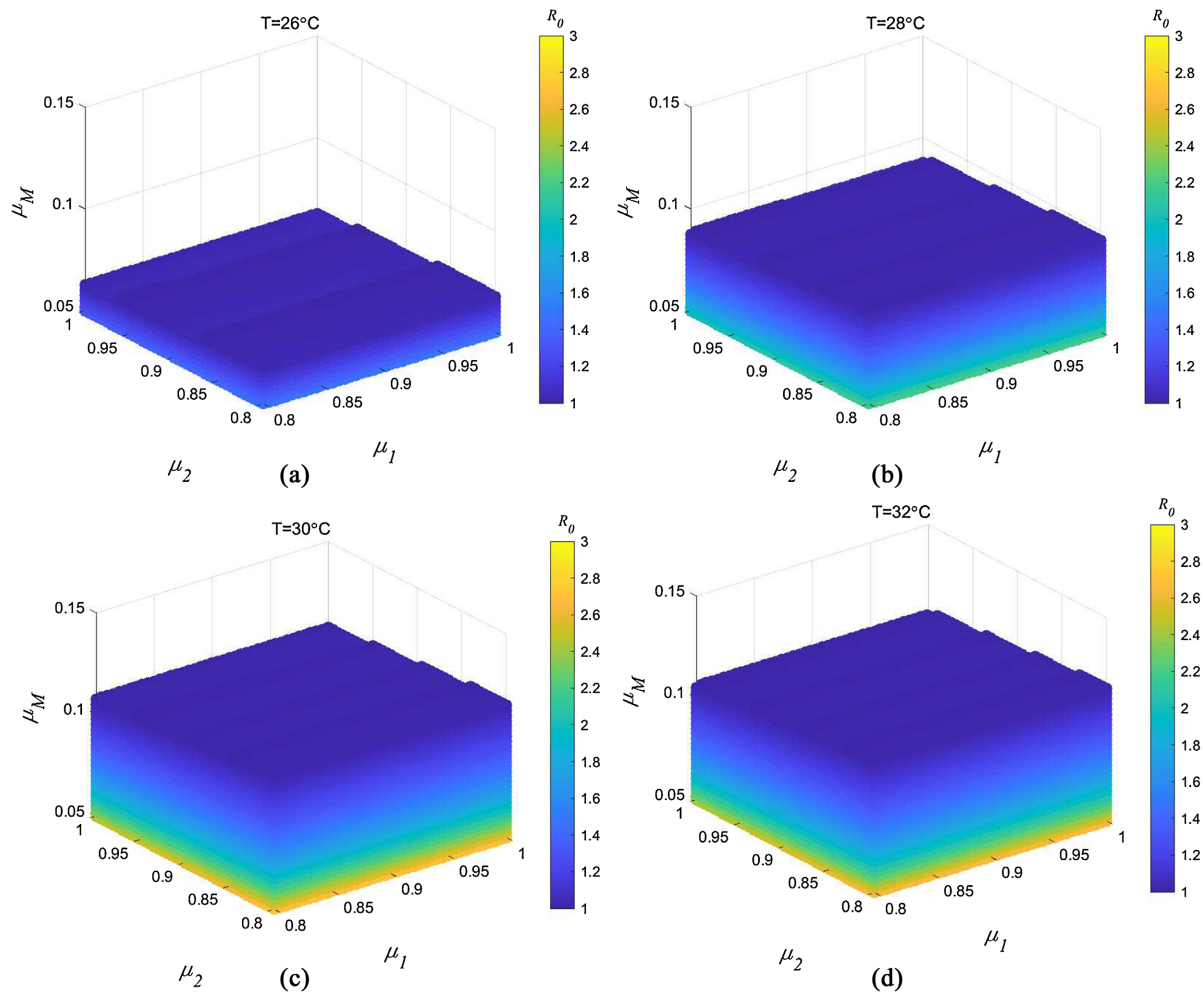


Figure 22. The effect of temperature and μ_i , μ_M together on R_0 : where the white part indicates that $R_0 < 1$ when the parameter is in the region, and the rest of the colored part indicates the case where $R_0 > 1$. (a) $T = 26^\circ\text{C}$; (b) $T = 28^\circ\text{C}$; (c) $T = 30^\circ\text{C}$; (d) $T = 32^\circ\text{C}$.

new tool for mosquito vector control [30]-[32]. This technique can reduce the reliance on chemical insecticides. As previously analyzed, controlling Zika virus requires a high mortality rate for mosquitoes. However, the extensive use of chemical insecticides not only pollutes the environment but also leads to insecticide resistance. SIT works by releasing sterilized male mosquitoes to suppress the reproduction of the same species, thereby reducing the overall mosquito population. This technique has already undergone field trials in several countries and has demonstrated significant suppression results [33]-[36]. According to our model, if the mosquito population is reduced by 20%, the temperature range where the R_0 is greater than 1 will shrink by 0.54°C , and the peak will decrease by about 10.297% (see Figure 23(a)). If mosquito populations are reduced to 50% of their current levels, the future risk of transmission could decrease by 29.422% (see Figure 23(b)). If the mosquito population is reduced by 80%, even in tropical

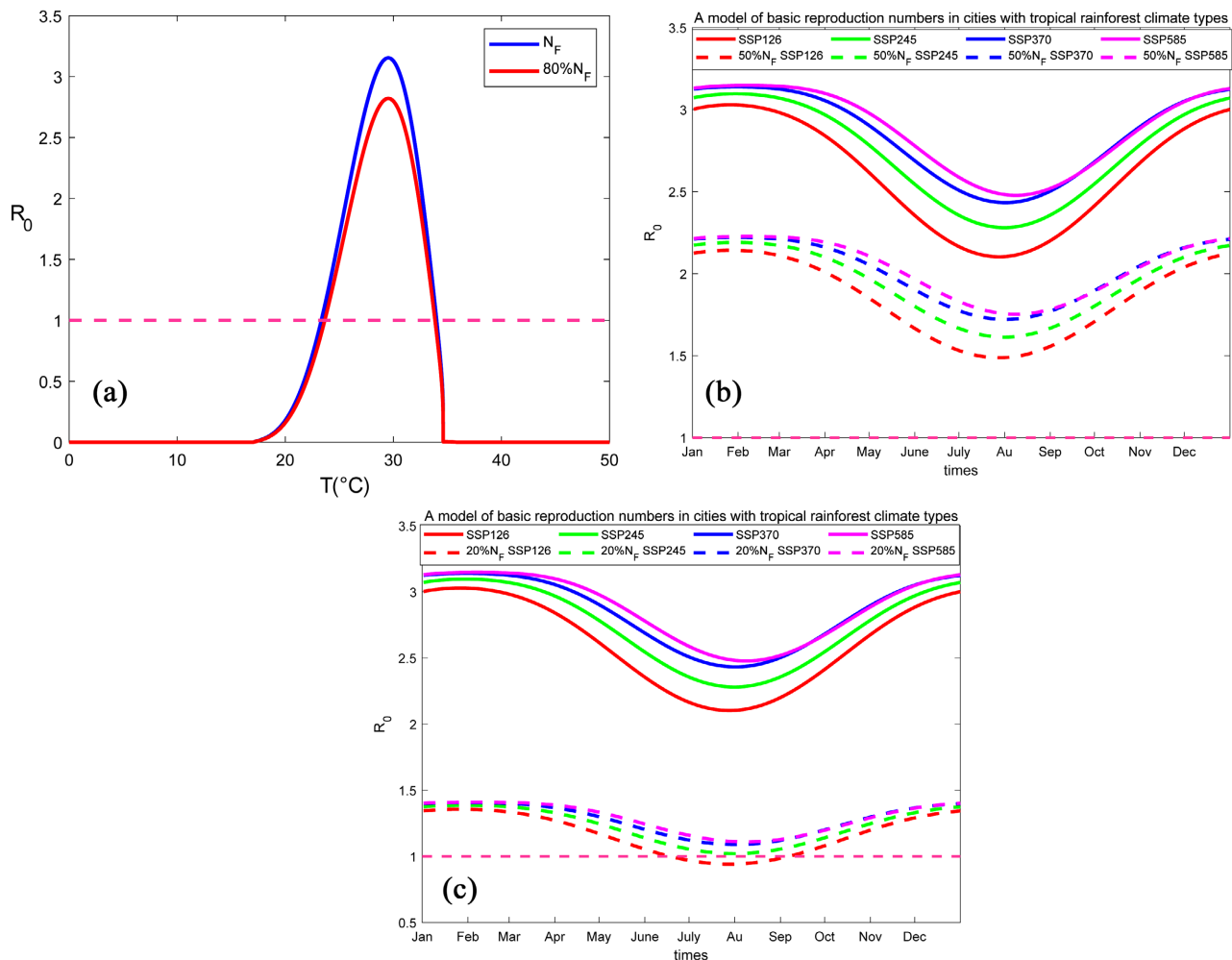


Figure 23. Effect of reducing the number of female mosquitoes (N_F) on R_0 . (a) The number of mosquitoes decreased by 20% and R_0 varies with temperature. (b) The basic reproduction number model for tropical rainforest climate cities in 2060-2070 when the mosquito population is reduced by 50%. (c) The basic reproduction number model for tropical rainforest climate cities in 2060-2070 when the mosquito population is reduced by 80%.

rainforest climates, Zika virus will only remain at a low transmission level in the future (see **Figure 23(c)**). Compared to other measures, this approach is more effective.

5. Discussion

Mordecai *et al.* [14] used a basic reproduction number model based on parameter significance assumptions [37] to predict the impact of temperature on the transmission probability and intensity of Zika virus, chikungunya, and dengue, finding that transmission occurs between 18°C-34°C, with the peak transmission occurring between 26°C-29°C. Tesla *et al.* [9] updated the previous basic reproduction number model by using experimental data and a generalized linear model to estimate the thermal response functions of vector competence parameters, determining that the optimal temperature for Zika virus transmission is 29°C, with a range of 22.7°C-34.7°C. Van Wyk *et al.* [11] built upon Tesla *et al.* [9]'s thermal response functions and incorporated a general compartmental model for dengue and Zika virus to calculate the basic reproduction number, estimating that the optimal temperature for Zika virus transmission is 30.5°C, with a range of 25.1°C-34.9°C. This indicates that the optimal transmission temperature and the minimum temperature for transmission estimated using the general compartmental model are higher than previous estimates. However, this study employs a compartmental model specifically designed for the transmission characteristics of Zika virus. Based on this model, the estimated basic reproduction number suggests that the optimal temperature for Zika virus transmission is 29.4°C, with a transmission range of 23.34°C-33.99°C. Compared to the results of Van Wyk *et al.* [11], the temperatures are lower, particularly the optimal transmission temperature, which is closer to [9]'s estimate. The minimum transmission temperature is also lower than Tesla *et al.* [9]'s estimate, but still within the range estimated by Mordecai *et al.* [14]. This suggests that the basic reproduction number obtained from a general model may underestimate the risk of Zika virus transmission.

By incorporating seasonality into the model, we divided ten Brazilian cities into five different climate zones based on seasonal variations. Using historical average temperatures from these regions, we compared and analyzed the timing of prevention and control measures and the risk of Zika virus transmission in different areas. Additionally, we developed a risk prediction model using future temperature projections under different Shared Socioeconomic Pathways (SSP126, SSP245, SSP370, SSP585) to forecast the risk of Zika virus outbreaks in 2060-2070. Based on SSP126, we created a Zika virus risk map for Brazil, highlighting areas of concern for each month. The study indicates that Zika virus risk varies across regions at the same time and that, with rising future temperatures, the duration of control periods in the same region will extend. For tropical savanna cities, the future Zika virus risk period ($R_0 > 1$) will increase by approximately 53 days compared to the present. Subtropical climate cities will see their risk period increase by about 70 days. Tropical climate cities will experience an increase of about 85

days in Zika virus risk in the future. Tropical savanna and tropical monsoon climate cities face year-round risk, with future annual R_0 significantly increasing, indicating that much stronger prevention and control efforts will be needed for Zika virus in the future.

It is important to note that the spread of Zika virus is not necessarily stronger at higher temperatures. For example, the increase in the basic reproduction number in savanna cities is not consistent with the temperature model (Figure 15). Specifically, during the period from November to March, when temperatures increase, the basic reproduction number actually decreases. The fluctuation of the basic reproduction number at the highest temperatures in January shows a local minimum value. This suggests that when temperatures rise to a certain threshold, it does not lead to further spread of Zika virus and may even inhibit it. This could be due to the fact that extremely high temperatures are not conducive to mosquito growth, thus hindering the spread of Zika virus.

Through a sensitivity analysis of control parameters under different temperatures, we found that the human-to-mosquito infection rate, mosquito mortality rate, and mosquito population size exhibit high sensitivity to the basic reproduction number (R_0). As temperature changes, effective virus control requires continuous adjustment of these parameters. Notably, sensitivity analysis, particularly PRCC analysis, shows that β_H (human-to-mosquito transmission rate) is more sensitive than β_M (mosquito-to-human transmission rate), indicating that vaccination is more effective than physical protection. However, focusing solely on traditional control methods, it is clear that as global temperatures rise, achieving control over the Zika virus requires a higher mosquito mortality rate. Considering the limitations and unsustainability of chemical insecticides, we compared the effectiveness of SIT. The results show that reducing the mosquito population by 80% using SIT can significantly reduce future Zika virus transmission, lowering the risk by approximately 55.2196%.

It is important to note that the dengue virus and chikungunya virus, which co-exist with the Zika virus, are also transmitted by *Aedes* mosquitoes. Although this paper focuses on the Zika virus, the same methods can be applied to further predict the transmission and risks of dengue and chikungunya viruses. Notably, the control methods for these viruses are similar, making SIT a promising long-term solution. However, determining the optimal level of mosquito population suppression to ensure effective virus control without causing issues like population replacement remains an area that requires further study.

In conclusion, although our current research has achieved some progress in understanding the transmission of Zika virus in the context of temperature, there is still a long way to go to fully elucidate its complex mechanisms and develop effective strategies to curb the spread of this pathogen. Meanwhile, it is rather rough that we rely on a simple cosine function to simulate the seasonal variation of temperature. In the future, I plan to incorporate stochastic fluctuations into the model to make it more realistic. We hope that this research will serve as a

foundation for further studies and encourage other researchers to address the remaining open problems.

Acknowledgements

The work is supported by Natural Science Foundation of Shaanxi Province(2023-JC-YB-084).

Author Contributions Statement

Zongmin Yue: Writing, Review, Supervision, Formal analysis, Methodology, Conceptualization. **Xiangrui Ji:** Writing original draft, Methodology, Investigation, and Formal analysis. **Yingpan zhang:** Editing, Formal analysis.

Data Availability

All data generated or analyzed during this study are included in this article, and the original data sources are cited through references and URLs.

Conflicts of Interest

The authors declare no conflicts of interest regarding the publication of this paper.

References

- [1] Sadeghieh, T., Sargeant, J.M., Greer, A.L., Berke, O., Dueymes, G., Gachon, P., *et al.* (2021) Zika Virus Outbreak in Brazil under Current and Future Climate. *Epidemics*, **37**, Article 100491. <https://doi.org/10.1016/j.epidem.2021.100491>
- [2] WHO (2016) Who to Convene an International Health Regulations Emergency Committee on Zika Virus and Observed Increase in Neurological Disorders and Neonatal Malformations. <https://www.who.int/news/item/28-01-2016-who-to-convene-an-international-health-regulations-emergency-committee-on-zika-virus-and-observed-increase-in-neurological-disorders-and-neonatal-malformations#:~:text=WHO%20Director-General%2C%20Margaret%20Chan%2C%20will%20convene%20an%20International.0bserved%20increase%20in%20neurological%20disorders%20and%20neonatal%20malformations>
- [3] Wang, L., Jia, Q., Zhu, G., Ou, G. and Tang, T. (2024) Transmission Dynamics of Zika Virus with Multiple Infection Routes and a Case Study in Brazil. *Scientific Reports*, **14**, Article No. 7424. <https://doi.org/10.1038/s41598-024-58025-7>
- [4] Fay, R.L., Cruz-Loya, M., Keyel, A.C., Price, D.C., Zink, S.D., Mordecai, E.A., *et al.* (2024) Population-Specific Thermal Responses Contribute to Regional Variability in Arbovirus Transmission with Changing Climates. *iScience*, **27**, Article 109934. <https://doi.org/10.1016/j.isci.2024.109934>
- [5] Dahlin, K.J.-M., O'Regan, S.M., Han, B.A., Schmidt, J.P. and Drake, J.M. (2024) Impacts of Host Availability and Temperature on Mosquito-Borne Parasite Transmission. *Ecological Monographs*, **94**, e1603. <https://doi.org/10.1002/ecm.1603>
- [6] Shocket, M., Ryan, S. and Mordecai, E. (2018) Temperature Explains Broad Patterns of Ross River Virus Transmission. *elifé*, **7**, e37762. <https://doi.org/10.7554/eLife.37762>
- [7] Ryan, S.J., Carlson, C.J., Mordecai, E.A. and Johnson, L.R. (2017) Global Expansion

- and Redistribution of Aedes-Borne Virus Transmission Risk with Climate Change. *PLOS Neglected Tropical Diseases*, **13**, e0007213. <https://doi.org/10.1371/journal.pntd.0007213>
- [8] Carlson, C.J., Dougherty, E.R. and Getz, W. (2016) An Ecological Assessment of the Pandemic Threat of Zika Virus. *PLOS Neglected Tropical Diseases*, **10**, e0004968. <https://doi.org/10.1371/journal.pntd.0004968>
- [9] Tesla, B., Demakovsky, L.R., Mordecai, E.A., Ryan, S.J., Bonds, M.H., Ngonghala, C.N., *et al.* (2018) Temperature Drives Zika Virus Transmission: Evidence from Empirical and Mathematical Models. *Proceedings of the Royal Society B: Biological Sciences*, **285**, Article 20180795. <https://doi.org/10.1098/rspb.2018.0795>
- [10] Huber, J.H., Childs, M.L., Caldwell, J.M. and Mordecai, E.A. (2017) Seasonal Temperature Variation Influences Climate Suitability for Dengue, Chikungunya, and Zika Transmission. *PLOS Neglected Tropical Diseases*, **12**, e0006451. <https://doi.org/10.1371/journal.pntd.0006451>
- [11] Van Wyk, H., Eisenberg, J.N.S. and Brouwer, A.F. (2023) Long-Term Projections of the Impacts of Warming Temperatures on Zika and Dengue Risk in Four Brazilian Cities Using a Temperature-Dependent Basic Reproduction Number. *PLOS Neglected Tropical Diseases*, **17**, e0010839. <https://doi.org/10.1371/journal.pntd.0010839>
- [12] Pielnaa, P., Al-Saadawe, M., Saro, A., Dama, M.F., Zhou, M., Huang, Y., *et al.* (2020) Zika Virus-Spread, Epidemiology, Genome, Transmission Cycle, Clinical Manifestation, Associated Challenges, Vaccine and Antiviral Drug Development. *Virology*, **543**, 34-42. <https://doi.org/10.1016/j.virol.2020.01.015>
- [13] Du, S., Liu, Y., Liu, J., Zhao, J., Champagne, C., Tong, L., *et al.* (2019) Aedes Mosquitoes Acquire and Transmit Zika Virus by Breeding in Contaminated Aquatic Environments. *Nature Communications*, **10**, Article No. 1324. <https://doi.org/10.1038/s41467-019-09256-0>
- [14] Mordecai, E.A., Cohen, J.M., Evans, M.V., Gudapati, P., Johnson, L.R., Lippi, C.A., *et al.* (2017) Detecting the Impact of Temperature on Transmission of Zika, Dengue, and Chikungunya Using Mechanistic Models. *PLOS Neglected Tropical Diseases*, **11**, e0005568. <https://doi.org/10.1371/journal.pntd.0005568>
- [15] van den Driessche, P. and Watmough, J. (2002) Reproduction Numbers and Sub-Threshold Endemic Equilibria for Compartmental Models of Disease Transmission. *Mathematical Biosciences*, **180**, 29-48. [https://doi.org/10.1016/s0025-5564\(02\)00108-6](https://doi.org/10.1016/s0025-5564(02)00108-6)
- [16] Manore, C.A., Hickmann, K.S., Xu, S., Wearing, H.J. and Hyman, J.M. (2014) Comparing Dengue and Chikungunya Emergence and Endemic Transmission in A. Aegypti and A. Albopictus. *Journal of Theoretical Biology*, **356**, 174-191. <https://doi.org/10.1016/j.jtbi.2014.04.033>
- [17] WHO (2022) Zika Virus. <https://www.who.int/news-room/fact-sheets/detail/zika-virus>
- [18] Curado, L.F.A., de Paulo, S.R., de Paulo, I.J.C., de Oliveira Maionchi, D., da Silva, H.J.A., de Oliveira Costa, R., *et al.* (2023) Trends and Patterns of Daily Maximum, Minimum and Mean Temperature in Brazil from 2000 to 2020. *Climate*, **11**, Article 168. <https://doi.org/10.3390/cli11080168>
- [19] Ferguson, N.M., Cucunubá, Z.M., Dorigatti, I., Nedjati-Gilani, G.L., Donnelly, C.A., Basáñez, M., *et al.* (2016) Countering the Zika Epidemic in Latin America. *Science*, **353**, 353-354. <https://doi.org/10.1126/science.aag0219>

- [20] DataBank (2023) Brazil. <https://data.worldbank.org.cn/indicator/SP.POP.TOTL?locations=BR>
- [21] Aidoni, A., Kofidis, K., Cocianu, C.L. and Avram, L. (2023) Deep Learning Models for Natural Gas Demand Forecasting: A Comparative Study of MLP, CNN, and LSTM. *Romanian Journal of Petroleum & Gas Technology*, **4**, 133-148. <https://doi.org/10.51865/jpgt.2023.01.12>
- [22] Arriola, L. and Hyman, J.M. (2009) Sensitivity Analysis for Uncertainty Quantification in Mathematical Models. In: Chowell, G., Hyman, J.M., Bettencourt, L.M.A. and Castillo-Chavez, C., Eds., *Mathematical and Statistical Estimation Approaches in Epidemiology*, Springer, 195-247. https://doi.org/10.1007/978-90-481-2313-1_10
- [23] Marino, S., Hogue, I.B., Ray, C.J. and Kirschner, D.E. (2008) A Methodology for Performing Global Uncertainty and Sensitivity Analysis in Systems Biology. *Journal of Theoretical Biology*, **254**, 178-196. <https://doi.org/10.1016/j.jtbi.2008.04.011>
- [24] Ltd Shanghai 2345 Network Technology Co. (n.d.) 2345 Weather Forecast Official Website. <https://tianqi.2345.com>
- [25] Zhou, T., Zou, L. and Chen, X. (2019) Commentary on the Coupled Model Intercomparison Project Phase 6. *Climate Change Research*, **15**, 445-456. <http://www.climatechange.cn/CN/10.12006/j.issn.1673-1719.2019.193>
- [26] Kutner, M. (1974) *Applied Linear Statistical Models*. McGraw Hill.
- [27] Lakhani, K.H. and Service, M.W. (1974) Estimated Mortalities of the Immature Stages of *Aedes cantans* (Mg.) (Diptera, Culicidae) in a Natural Habitat. *Bulletin of Entomological Research*, **64**, 265-276. <https://doi.org/10.1017/s0007485300031151>
- [28] Thériault, R., Ben-Shachar, M.S., Patil, I. Lüdecke, D., Wiernik, B.M. and Makowski, D. (2023) Check Your Outliers! An Introduction to Identifying Statistical Outliers in R with *easystats*. *Behavior Research Methods*, **56**, 4162-4172. <https://doi.org/10.3758/s13428-024-02356-w>
- [29] Beck, H.E., Zimmermann, N.E., McVicar, T.R., Vergopolan, N., Berg, A. and Wood, E.F. (2018) Present and Future Köppen-Geiger Climate Classification Maps at 1-km Resolution. *Scientific Data*, **5**, Article No. 180214. <https://doi.org/10.1038/sdata.2018.214>
- [30] Zhang, D., Maiga, H., Li, Y., Bakhoum, M.T., Wang, G., Sun, Y., et al. (1980) Mating Harassment May Boost the Effectiveness of the Sterile Insect Technique for *Aedes* Mosquitoes. *Nature Communications*, **15**, Article No. 1980. <https://doi.org/10.1038/s41467-024-46268-x>
- [31] Ferrater, J.B., Gómez-Marco, F., Yoshimoto, A.K., Greene, T.D., Simmons, G.S., Daugherty, M.P., et al. (2024) Development of a Sterile Insect Technique as a Control Strategy for the Asian Citrus Psyllid: Establishing the Effect of Sterilizing X-Rays on Fecundity, Fertility, and Survival. *Journal of Economic Entomology*, **117**, 1356-1366. <https://doi.org/10.1093/jee/toae098>
- [32] Kandul, N.P., Liu, J., Buchman, A., Shriner, I.C., Corder, R.M., Warsinger-Pepe, N., et al. (2022) Precision Guided Sterile Males Suppress Populations of an Invasive Crop Pest. *GEN Biotechnology*, **1**, 372-385. <https://doi.org/10.1089/genbio.2022.0019>
- [33] Tur, C., Almenar, D., Zacarés, M., Benlloch-Navarro, S., Pla, I. and Dalmau, V. (2023) Suppression Trial through an Integrated Vector Management of *Aedes albopictus* (Skuse) Based on the Sterile Insect Technique in a Non-Isolated Area in Spain. *Insects*, **14**, Article 688. <https://doi.org/10.3390/insects14080688>
- [34] Ranathunge, T., Harishchandra, J., Maiga, H., Bouyer, J., Gunawardena, Y.I.N.S. and Hapugoda, M. (2022) Development of the Sterile Insect Technique to Control the Dengue Vector *Aedes aegypti* (Linnaeus) in Sri Lanka. *PLOS ONE*, **17**, e0265244. <https://doi.org/10.1371/journal.pone.0265244>

- [35] Malinga, L. (2024) A Novel Approach to the Sterile Insect Technique (SIT) for Eldana Saccharina Management in South Africa. *Sugar Tech*, **26**, 629-634.
<https://doi.org/10.1007/s12355-024-01378-0>
- [36] Bliman, P.-A., Nguyen, N. and Vauchelet, N. (2024) Efficacy of the Sterile Insect Technique in the Presence of Inaccessible Areas: A Study Using Two-Patch Models. arXiv: 2403.20069. <https://doi.org/10.48550/arXiv.2403.20069>
- [37] Dietz, K. (1993) The Estimation of the Basic Reproduction Number for Infectious Diseases. *Statistical Methods in Medical Research*, **2**, 23-41.
<https://doi.org/10.1177/096228029300200103>